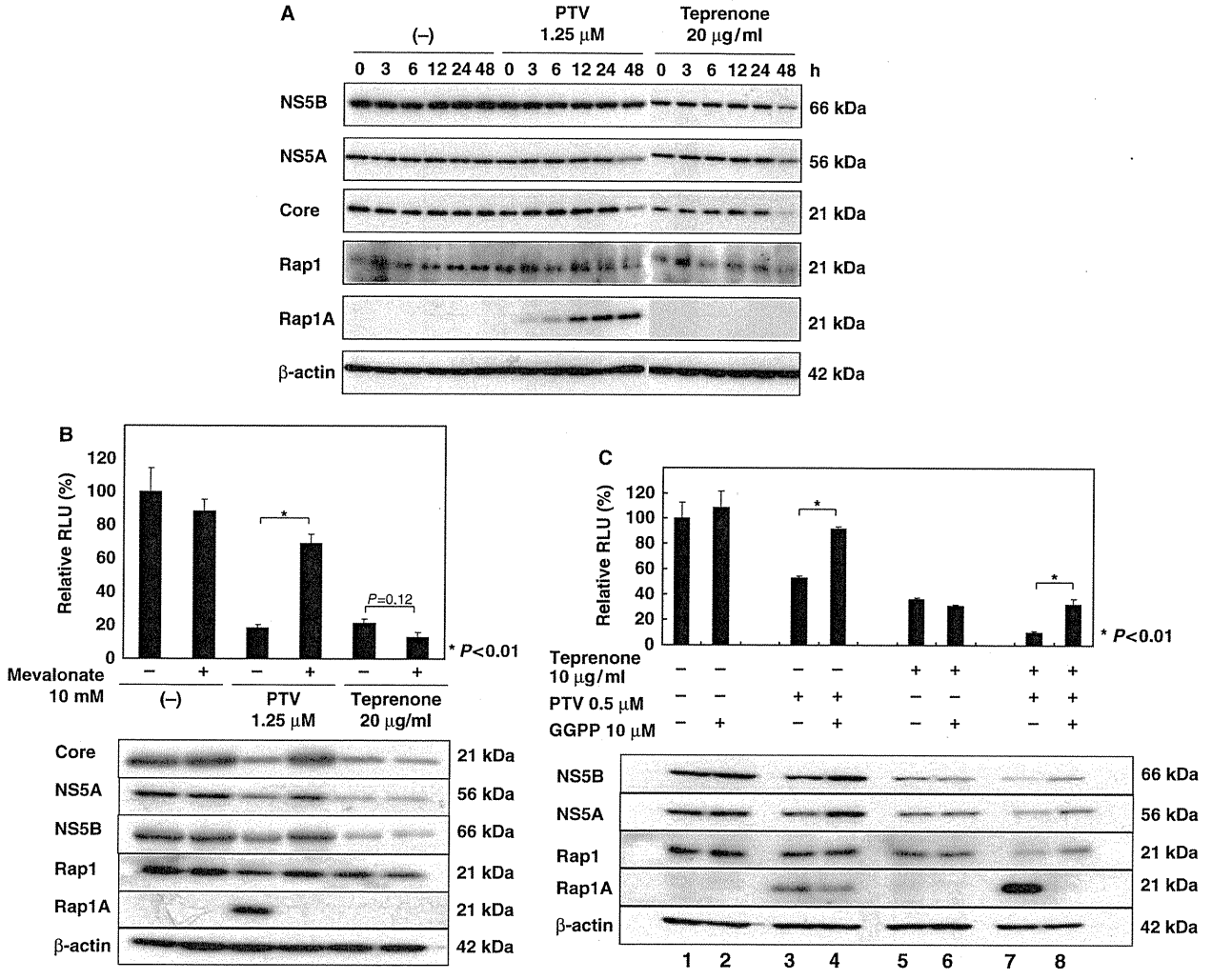

Fig. 6. Teprenone did not inhibit geranylgeranylation. (A) Teprenone did not inhibit geranylgeranylation. OR6 cells were treated with pitavastatin (PTV) (1.25 μM) or teprenone (20 μg/ml), or neither for 0, 3, 6, 12, 24 and 48 h. The cells were subjected to western blot analysis for HCV proteins using anti-NS5B, anti-NS5A and anti-Core antibodies, and for geranylgeranylation assay using anti-Rap1A (sc-1482) and anti-Rap1 (sc-65) antibodies. (B) Mevalonate did not affect the anti-HCV activity of teprenone. OR6 cells were treated with PTV (1.25 μM), teprenone (20 μg/ml) or neither in the absence or in the presence of mevalonate (10 mM) for 72 h. Then the cells were subjected to luciferase assay (upper panel) and western blot analysis using anti-Core, anti-NS5A, anti-NS5B, anti-Rap1A (sc-1482), anti-Rap1 (sc-65) and anti-β-actin antibodies (lower panel), as shown in (A). (C) Teprenone was not used as a substrate for GGT after the depletion of geranylgeranyl pyrophosphate (GGPP) by statin. OR6 cells were treated with teprenone (0 and 10 μg/ml), PTV (0 and 0.5 μM) and GGPP (0 and 10 μM) in the indicated combination for 72 h. Then the cells were subjected to luciferase assay (upper panel) and geranylgeranyl assay using anti-Rap1A (sc-1482) and anti-Rap1 (sc-65) antibodies (lower panel) as shown in (A).

suggest that teprenone enhances statins' inhibitory action against geranylgeranylation, except for PRV.

Discussion

In this study, we demonstrated that teprenone inhibited HCV RNA replication. Furthermore, teprenone exhibited anti-HCV activity in the genotype-2a JFH-1 infection system. Teprenone belongs to the geranyl compounds from its chemical structure and anti-ulcer agent from its clinical application. Therefore, we tested other geranyl compounds (GGOH and VK2, as well as geranylgeranoic acid) and other anti-ulcer agents (ecabet sodium, sofalcone and gefarnate) for their effect on HCV RNA replication. However, only teprenone exhibited anti-HCV activity among the reagents tested. Therefore, the anti-HCV activity of teprenone is a unique feature among these reagents.

The interview form from Selbex providing company Eisai reported the plasma concentration of teprenone. When 150 mg of Selbex was administered orally, its maximum plasma concentration reached 2.2 μg/ml. This is similar to the EC_{50} (5.3 μg/ml) of Selbex *in vitro*.

Ichikawa *et al.* (23) reported that teprenone induced the 2′,5′-oligoadenylate synthetases (2′5′-OAS) in

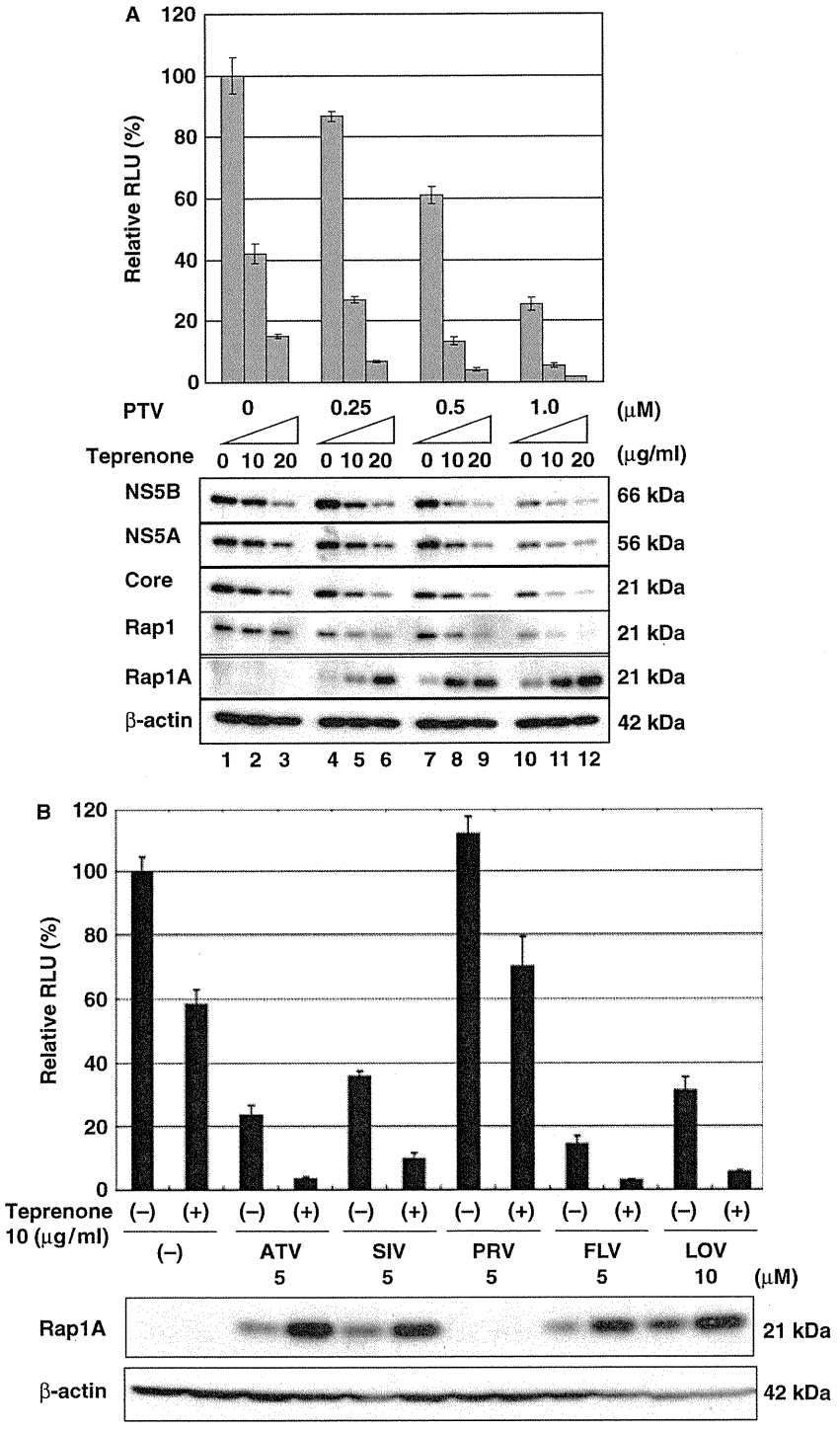

Fig. 7. Teprenone enhanced statins' inhibitory action against geranylgeranylation. (A) Teprenone enhanced pitavastatin (PTV)'s inhibitory action against geranylgeranylation. OR6 cells were treated with teprenone (0, 10 and 20 μg/ml) and PTV (0, 0.25, 0.5 and 1.0 μM) for 72 h. Then the cells were subjected to luciferase assay (upper panel) and western blot analysis using anti-NS5A, anti-Rap1A (sc-1482) and anti-Rap1 (sc-65), and anti-β-actin antibodies (lower panel), as shown in Figure 6A. (B) Teprenone enhanced statins' [except for pravastatin (PRV)] inhibitory action against geranylgeranylation. OR6 cells were treated with teprenone (0, 10 μg/ml) and atorvastatin (0, 5 μM), simvastatin (0, 5 μM), PRV (0, 5 μM), fluvastatin (0, 5 μM) and lovastatin (0, 10 μM) for 72 h. Then the cells were subjected to luciferase assay (upper panel) and western blot analysis using anti-Rap1A (sc-1482), and anti-β-actin antibodies (lower panel), as shown in Figure 6A.

Liver International (2011)

human hepatoma cells. We demonstrated the activation of 2′5′-OAS and IFN-stimulated response element (ISRE) by IFN-α using the reporter assay system in our HuH-7-derived OR6 cells. However, we could not obtain evidence that teprenone activated both 2′5′-OAS and ISRE promoters (supporting information, Fig. S2A and B). Signal transducer and activator of transcription (STAT)1 and STAT2 were not phosphorylated after treatment with teprenone (supporting information, Fig. S2C). This discrepancy may have been caused by the heterogeneity of HuH-7 cells, because OR6 was selected as the clonal cell line and is highly susceptible to HCV RNA replication. Further study is needed to clarify the mechanism underlying teprenone's effect on IFN signalling.

Teprenone reportedly protects the gastric mucosa by inducing HSP (24). From this standpoint, the anti-HCV activity of teprenone was an unexpected result, because recently, it was reported that HSP90 is essential for HCV RNA replication and that an HSP90 inhibitor, geldanamycin, inhibits HCV RNA replication (25, 26). We examined whether or not teprenone induced HSP90 in hepatoma cells and found that it did not (supporting information, Fig. S4).

In this study, we monitored the geranylgeranylated state of Rap1A as a marker using nongeranylgeranylated Rap1A-detectable anti-Rap1A antibody (sc-1482). The least expected result of this sensitive geranylgeranylation assay is that teprenone enhanced statins' inhibitory action against geranylgeranylation. It is not clear in this study as to why teprenone enhanced statins' inhibitory action on geranylgeranylation. One possibility is that teprenone may cause biosynthesis from FPP to cholesterol rather than to GGPP by an unknown mechanism. To clarify this point, further study will be needed. This new function of teprenone may contribute to not only the antiviral field but also other fields, including studies on osteoporosis and on various kinds of antitumours, because geranylgeranylation and farnesylation are targets of the reagent in these fields. For example, statins interfere with the production of GGPP and FPP, which is important in the activation of small G proteins, such as K-ras and the Rho family, and disrupt the growth of malignant cells.

Recently, two important findings have been reported. Firstly, El-Serag *et al.* (8) reported that statins are associated with a reduced risk of HCC. Secondly, Abraldes *et al.* (9) reported that statin lowers portal pressure in patients with cirrhosis. Therefore, as teprenone is a strong adjuvant to statin's inhibitory action against geranylgeranylation, it may further improve portal hypertension in cirrhosis and reduce the risk of HCC in combination with statins. Although teprenone alone possesses modest anti-HCV activity, it will play a significant role in combination with IFN and/or statins in the therapy to HCV-associated liver diseases as an adjuvant like ribavirin. As teprenone is available in clinical use with a low side effect, a clinical study using teprenone in combination with IFN-α and/or statins is now underway in our institution.

In conclusion, we have shown that the anti-ulcer agent teprenone inhibited HCV RNA replication and enhanced statins' inhibitory action against geranylgeranylation. This newly discovered function of teprenone may contribute to improve the treatment of HCV-associated liver diseases (CH C, cirrhosis and HCC) as an adjuvant to statins.

Acknowledgements

The authors would like to thank Atsumi Morishita, Takashi Nakamura and Midori Takeda for their technical assistance. This work was supported by grants-in-aid for a third-term comprehensive 10-year strategy for cancer control and for research on hepatitis from the Ministry of Health, Labor, and Welfare of Japan. K. A. and K. M. were supported by a Research Fellowship from the Japan Society for the Promotion of Science (JSPS) for Young Scientists.

References

1. Feld JJ, Hoofnagle JH. Mechanism of action of interferon and ribavirin in treatment of hepatitis C. *Nature* 2005; **436**: 967–72.
2. Ikeda M, Abe K, Dansako H, *et al.* Efficient replication of a full-length hepatitis C virus genome, strain O, in cell culture, and development of a luciferase reporter system. *Biochem Biophys Res Commun* 2005; **329**: 1350–9.
3. Ikeda M, Abe K, Yamada M, *et al.* Different anti-HCV profiles of statins and their potential for combination therapy with interferon. *Hepatology* 2006; **44**: 117–25.
4. Ikeda M, Kato N. Modulation of host metabolism as a target of new antivirals. *Adv Drug Deliv Rev* 2007; **59**: 1277–89.
5. Ikeda M, Kato N. Life style-related diseases of the digestive system: cell culture system for the screening of anti-hepatitis C virus HCV reagents: suppression of HCV replication by statins and synergistic action with interferon. *J Pharmacol Sci* 2007; **105**: 145–50.
6. Kim SS, Peng LF, Lin W, *et al.* A cell-based, high-throughput screen for small molecule regulators of hepatitis C virus replication. *Gastroenterology* 2007; **132**: 311–20.
7. Bader T, Fazili J, Madhoun M, *et al.* Fluvastatin inhibits hepatitis C replication in humans. *Am J Gastroenterol* 2008; **103**: 1383–9.
8. El-Serag HB, Johnson ML, Hachem C, Morgana RO. Statins are associated with a reduced risk of hepatocellular carcinoma in a large cohort of patients with diabetes. *Gastroenterology* 2009; **136**: 1601–8.
9. Abraldes JG, Albillos A, Banares R, *et al.* Simvastatin lowers portal pressure in patients with cirrhosis and portal hypertension: a randomized controlled trial. *Gastroenterology* 2009; **136**: 1651–8.

10. Kapadia SB, Chisari FV. Hepatitis C virus RNA replication is regulated by host geranylgeranylation and fatty acids. *Proc Natl Acad Sci USA* 2005; **102**: 2561–6.
11. Ye J, Wang C, Sumpter R Jr, *et al.* Disruption of hepatitis C virus RNA replication through inhibition of host protein geranylgeranylation. *Proc Natl Acad Sci USA* 2003; **100**: 15865–70.
12. Wang C, Gale M Jr, Keller BC, *et al.* Identification of FBL2 as a geranylgeranylated cellular protein required for hepatitis C virus RNA replication. *Mol Cell* 2005; **18**: 425–34.
13. Lindenbach BD, Evans MJ, Syder AJ, *et al.* Complete replication of hepatitis C virus in cell culture. *Science* 2005; **309**: 623–6.
14. Wakita T, Pietschmann T, Kato T, *et al.* Production of infectious hepatitis C virus in tissue culture from a cloned viral genome. *Nat Med* 2005; **11**: 791–6.
15. Zhong J, Gastaminza P, Cheng G, *et al.* Robust hepatitis C virus infection in vitro. *Proc Natl Acad Sci USA* 2005; **102**: 9294–9.
16. Nanke Y, Kotake S, Ninomiya T, *et al.* Geranylgeranylacetone inhibits formation and function of human osteoclasts and prevents bone loss in tail-suspended rats and ovariectomized rats. *Calcif Tissue Int* 2005; **77**: 376–85.
17. Kato N, Sugiyama K, Namba K, *et al.* Establishment of a hepatitis C virus subgenomic replicon derived from human hepatocytes infected in vitro. *Biochem Biophys Res Commun* 2003; **306**: 756–66.
18. Naka K, Ikeda M, Abe K, Dansako H, Kato N. Mizoribine inhibits hepatitis C virus RNA replication: effect of combination with interferon-alpha. *Biochem Biophys Res Commun* 2005; **330**: 871–9.
19. Dansako H, Naganuma A, Nakamura T, *et al.* Differential activation of interferon-inducible genes by hepatitis C virus core protein mediated by the interferon stimulated response element. *Virus Res* 2003; **97**: 17–30.
20. Ariumi Y, Kuroki M, Abe K, *et al.* DDX3 DEAD-box RNA helicase is required for hepatitis C virus RNA replication. *J Virol* 2007; **81**: 13922–6.
21. Hughes A, Rogers MJ, Idris AI, Crockett JC. A comparison between the effects of hydrophobic and hydrophilic statins on osteoclast function in vitro and ovariectomy-induced bone loss in vivo. *Calcif Tissue Int* 2007; **81**: 403–1.
22. Merrell MA, Wakchoure S, Lehenkari PP, Harris KW, Selander KS. Inhibition of the mevalonate pathway and activation of p38 MAP kinase are independently regulated by nitrogen-containing bisphosphonates in breast cancer cells. *Eur J Pharmacol* 2007; **570**: 27–37.
23. Ichikawa T, Nakao K, Nakata K, *et al.* Geranylgeranylacetone induces antiviral gene expression in human hepatoma cells. *Biochem Biophys Res Commun* 2001; **280**: 933–9.
24. Hirakawa T, Rokutan K, Nikawa T, Kishi K. Geranylgeranylacetone induces heat shock proteins in cultured guinea pig gastric mucosal cells and rat gastric mucosa. *Gastroenterology* 1996; **111**: 345–57.
25. Nakagawa S, Umehara T, Matsuda C, *et al.* Hsp90 inhibitors suppress HCV replication in replicon cells and humanized liver mice. *Biochem Biophys Res Commun* 2007; **353**: 882–8.
26. Okamoto T, Nishimura Y, Ichimura T, *et al.* Hepatitis C virus RNA replication is regulated by FKBP8 and Hsp90. *Embo J* 2006; **25**: 5015–25.

Supporting information

Additional supporting information may be found in the online version of this article:

Fig. S1. The effects of anti-ulcer agents on HCV RNA replication. (A) Cell proliferation assay. OR6 cells were treated with teprenone (0, 2.5, 5, 10, and 20 μg/ml), and the cells at 24, 48, and 72 hours after treatment were subjected to WST-1 cell proliferation assay. (B) Structures of ant-ulcer agents. (C-E) OR6 cells were treated with ecabet sodium (0, 2.5, 5, 10, 20 μg/ml) (C), sofalcon (0, 2.5, 5, 10, 20 μg/ml) (D), and gefarnate (0, 2.5, 5, 10, 20 μg/ml) (E) for 72 hours. Then the cells were subjected to luciferase assay (upper panel) and Western blot analysis using anti-core, and anti-β-actin antibodies (lower panel) as shown in Figure 1B.

Fig. S2. Teprenone didn't activate IFN signaling pathway. (A and B) Luciferase assays for 2'5'OAS and ISRE promoters. p2'5'OAS-luc (A) and pISRE-luc (B) transfected OR6c cells were treated with teprenone (0, 2.5, 5, and 10 μg/ml) or IFN-α (0, 2.5, 5, and 10 IU/ml) for 6 hours and then subjected to luciferase reporter assay. (C) Teprenone didn't activate STATs in OR6 cells. OR6 cells were treated with IFN-α (500 IU/ml), PTV (1.25 μM), and teprenone (20 μg/ml) for 0, 3, 6, and 12 hours. Then the cells were subjected to Western blot analysis using anti-pSTAT1 (Tyr701), anti-STAT1, anti-pSTAT2 (Tyr689), anti-core, and anti-β-actin antibodies.

Fig. S3. Teprenone treatment didn't cause positive feedback of HMG-CoA reductase (HMGCR). OR6c cells were treated with teprenone (20 μg/ml), PTV (10 μmol/L), or neither for 24 hours. The cells were subjected to RT-PCR (A) and real-time RT-quantitative PCR (B) using HMG-CoA reductase-specific primer set. H_2O was used as a negative control. GAPDH was used as an internal control.

Fig. S4. Teprenone didn't induce HSP90 or HSP70 in HuH-7 cells. OR6 cells were treated with teprenone (20 μg/ml) for 0, 3, 6, 12, 24, and 48 hours. Then the cells were subjected to Western blot analysis using anti-HSP90, anti-HSP70 anti-core, and anti-β-actin antibodies.

Please note: Wiley-Blackwell is not responsible for the content or functionality of any supporting materials supplied by the authors. Any queries (other than missing material) should be directed to the corresponding author for the article.

Virus Genes
DOI 10.1007/s11262-012-0712-2

Development of a drug assay system with hepatitis C virus genome derived from a patient with acute hepatitis C

Kyoko Mori · Youki Ueda · Yasuo Ariumi · Hiromichi Dansako · Masanori Ikeda · Nobuyuki Kato

Received: 5 October 2011 / Accepted: 1 January 2012

Abstract We developed a new cell culture drug assay system (AH1R), in which genome-length hepatitis C virus (HCV) RNA (AH1 strain of genotype 1b derived from a patient with acute hepatitis C) efficiently replicates. By comparing the AH1R system with the OR6 assay system that we developed previously (O strain of genotype 1b derived from an HCV-positive blood donor), we demonstrated that the anti-HCV profiles of reagents including interferon-γ and cyclosporine A significantly differed between these assay systems. Furthermore, we found unexpectedly that rolipram, an anti-inflammatory drug, showed anti-HCV activity in the AH1R assay but not in the OR6 assay, suggesting that the anti-HCV activity of rolipram differs depending on the HCV strain. Taken together, these results suggest that the AH1R assay system is useful for the objective evaluation of anti-HCV reagents and for the discovery of different classes of anti-HCV reagents.

Keywords HCV · Acute hepatitis C · Anti-HCV drug assay system · Anti-HCV activity of rolipram

Introduction

Hepatitis C virus (HCV) infection frequently causes chronic hepatitis, which progresses to liver cirrhosis and hepatocellular carcinoma. HCV is an enveloped virus with a positive single-stranded 9.6 kb RNA genome, which encodes a large polyprotein precursor of approximately 3,000 amino acid (aa) residues [1, 2]. This polyprotein is cleaved by a combination of the host and viral proteases into at least 10 proteins in the following order: Core, envelope 1 (E1), E2, p7, non-structural 2 (NS2), NS3, NS4A, NS4B, NS5A, and NS5B [1].

Human hepatoma HuH-7 cell culture-based HCV replicon systems derived from a number of HCV strains have been widely used for various studies on HCV RNA replication [3, 4] since the first replicon system (based on the Con1 strain of genotype 1b) was developed in 1999 [5]. Genome-length HCV RNA replication systems (see Fig. 2 for details) derived from a limited number of HCV strains (H77, N, Con1, O, and JFH-1) are also sometimes used for such studies, as they are more useful than the replicon systems lacking the structural region of HCV, although the production of infectious HCV from the genome-length HCV RNA has not been demonstrated to date [3, 4]. Furthermore, these RNA replication systems have been improved enough to be suitable for the screening of anti-HCV reagents by the introduction of reporter genes such as luciferase [3, 4, 6]. We also developed an HuH-7-derived cell culture assay system (OR6) in which genome-length HCV RNA (O strain of genotype 1b derived from an HCV-positive blood donor) encoding renilla luciferase (RL) efficiently replicates [7]. Such reporter assay systems could save time and facilitate the mass screening of anti-HCV reagents, since the values of luciferase correlated well with the level of HCV RNA after treatment with anti-HCV reagents. Furthermore, OR6 assay system became more useful as a drug assay system than the HCV subgenomic replicon-based reporter assay systems developed to date [3, 4], because the older systems lack the Core-NS2 regions containing structural proteins likely to be involved in the events that take place in the HCV-infected human liver.

K. Mori · Y. Ueda · Y. Ariumi · H. Dansako · M. Ikeda · N. Kato (✉)
Department of Tumor Virology, Okayama University Graduate School of Medicine, Dentistry, and Pharmaceutical Sciences, 2-5-1 Shikata-cho, Okayama 700-8558, Japan
e-mail: nkato@md.okayama-u.ac.jp

Published online: 18 January 2012

Indeed, by the screening of preexisting drugs using the OR6 assay system, we have identified mizoribine [8], statins [9], hydroxyurea [10], and teprenone [11] as new anti-HCV drug candidates, indicating that the OR6 assay system is useful for the discovery of anti-HCV reagents.

On the other hand, we previously established for the first time an HuH-7-derived cell line (AH1) that harbors genome-length HCV RNA (AH1 strain of genotype 1b) derived from a patient with acute hepatitis C [12]. In that study, we noticed different anti-HCV profiles of interferon (IFN)-γ or cyclosporine A (CsA) between AH1 and O cells supporting genome-length HCV RNA (O strain) replication [7]. From these results, we supposed that the diverse effects of IFN-γ or CsA were attributable to the difference in HCV strains [12].

To test this assumption in detail, we first developed an AH1 strain-derived assay system (AH1R) corresponding to the OR6 assay system, and then performed a comparative analysis using AH1R and OR6 assay systems. In this article, we report that the difference in HCV strains causes the diverse effects of anti-HCV reagents, and we found unexpectedly by AH1R assay that rolipram, an anti-inflammatory drug, is an anti-HCV drug candidate.

Materials and methods

Reagents

IFN-α, IFN-γ, and CsA were purchased from Sigma-Aldrich (St. Louis, MO). Rolipram was purchased from Wako Pure Chemical Industries (Osaka, Japan).

Plasmid construction

The plasmid pAH1RN/C-5B/PL,LS,TA,$(VA)_3$ was constructed from pAH1 N/C-5B/PL,LS,TA,$(VA)_3$ encoding genome-length HCV RNA clone 2 (See Fig. 2) obtained from AH1 cells [12], by introducing a fragment of the RL gene from pORN/C-5B into the *Asc*I site before the neomycin phosphotransferase (Neo^R) gene as previously described [7].

RNA synthesis

The plasmid pAH1RN/C-5B/PL,LS,TA,$(VA)_3$ DNA was linearized by *Xba*I, and used for RNA synthesis with T7 MEGAscript (Ambion, Austin TX) as previously described [7].

Cell cultures

AH1R and OR6 cells supporting genome-length HCV RNAs were cultured in Dulbecco's modified Eagle's medium (DMEM) supplemented with 10% fetal bovine serum (FBS) and 0.3 mg/mL of G418 (Geneticin; Invitrogen, Carlsbad, CA). AH1c-cured cells, which were created by eliminating HCV RNA from AH1 cells [12] by IFN-γ treatment, were also cultured in DMEM supplemented with 10% FBS.

RNA transfection and selection of G418-resistant cells

Genome-length HCV (AH1RN/C-5B/PL,LS,TA,$(VA)_3$) RNA synthesized in vitro was transfected into AH1c cells by electroporation, and the cells were selected in the presence of G418 (0.3 mg/mL) for 3 weeks as described previously [13].

RL assay for anti-HCV reagents

To monitor the effects of anti-HCV reagents, RL assay was performed as described previously [14]. Briefly, the cells were plated onto 24-well plates (2×10^4 cells per well) in triplicate and cultured with the medium in the absence of G418 for 24 h. The cells were then treated with each reagent at several concentrations for 72 h. After treatment, the cells were subjected to a luciferase assay using the RL assay system (Promega, Madison, WI). From the assay results, the 50% effective concentration (EC_{50}) of each reagent was determined.

Quantification of HCV RNA

Quantitative reverse transcription-polymerase chain reaction (RT-PCR) analysis for HCV RNA was performed using a real-time LightCycler PCR (Roche Applied Science, Indianapolis, IN, USA) as described previously [7]. The experiments were done in triplicate.

IFN-α treatment to evaluate the assay systems

To monitor the anti-HCV effect of IFN-α on AH1R cells, 2×10^4 cells and 5×10^5 cells were plated onto 24-well plates (for luciferase assay) and 10 cm plates (for quantitative RT-PCR assay) in triplicate, respectively, and cultured for 24 h. The cells were then treated with IFN-α at final concentrations of 0, 1, 10, and 100 IU/mL for 24 h, and subjected to luciferase and quantitative RT-PCR assays as described above.

Western blot analysis

The preparation of cell lysates, sodium dodecyl sulfate–polyacrylamide gel electrophoresis, and immunoblotting analysis with a PVDF membrane were performed as described previously [13]. The antibodies used in this study were those against HCV Core (CP11 monoclonal antibody;

Institute of Immunology, Tokyo), NS5B, and E2 (generous gifts from Dr. M. Kohara, Tokyo Metropolitan Institute of Medical Science, Japan). Anti-β-actin antibody (AC-15; Sigma, St. Louis, MO, USA) was used as a control for the amount of protein loaded per lane. Immunocomplexes were detected with the Renaissance enhanced chemiluminescence assay (Perkin-Elmer Life Sciences, Boston, MA).

WST-1 cell proliferation assay

The cells were plated onto 96-well plates (1×10^3 cells per well) in triplicate and then treated with rolipram at several concentrations for 72 h. After treatment, the cells were subjected to the WST-1 cell proliferation assay (Takara Bio, Otsu, Japan) according to the manufacturer's protocol. From the assay results, the 50% cytotoxic concentration (CC_{50}) of rolipram was estimated. The selective index (SI) value of rolipram was also estimated by dividing the CC_{50} value by the EC_{50} value.

RT-PCR and sequencing

To amplify the genome-length HCV RNA, RT-PCR was performed separately in two fragments as described previously [7, 15]. Briefly, one fragment covered from 5′-untranslated region to NS3, with a final product of approximately 6.2 kb, and the other fragment covered from NS2 to NS5B, with a final product of approximately 6.1 kb. These fragments overlapped at the NS2 and NS3 regions and were used for sequence analysis of the HCV open reading frame (ORF) after cloning into pBR322MC. PrimScript (Takara Bio) and KOD-plus DNA polymerase (Toyobo, Osaka, Japan) were used for RT and PCR, respectively. The nucleotide sequences of each of the three independent clones obtained were determined using the Big Dye terminator cycle sequencing kit on an ABI PRISM 310 genetic analyzer (Applied Biosystems, Foster City, CA, USA).

Statistical analysis

Differences between AH1R and OR6 cell lines were tested using Student's t test. P values <0.05 were considered statistically significant.

Results

Development of a luciferase reporter assay system that facilitates the quantitative monitoring of genome-length HCV-AH1 RNA replication

To develop an HCV AH1 strain-derived assay system corresponding to the OR6 assay system [7], a genome-length HCV RNA encoding RL (AH1RN/C-5B/PL,LS,TA,$(VA)_3$) was transfected into AH1c cells. Following 3 weeks of culturing in the presence of G418, more than 10 colonies were obtained, and then 8 colonies (#2, #3, #4, #5, #6, #8, #13, and #14) were successfully proliferated. We initially selected colonies #2, #3, and #14 because they had high levels of RL activity (>4×10^6 U/1.6×10^5 cells) (Fig. 1a). However, RT-PCR and the sequencing analyses revealed that the genome-length HCV-AH1 RNAs obtained from these colonies each had an approximately 1 kb deletion in the E2 region (data not shown). In this regard, we previously observed similar phenomenon and described the difficulty of the development of a luciferase reporter assay system using the genome-length HCV RNA of more than 12 kb [7], suggesting that the NS5B polymerase possesses the limited elongation ability (probably up to a total length of 12 kb). Indeed, in that study, we could overcome this obstacle by the selection of the colony harboring a complete genome-length HCV RNA among the obtained G418-resistant colonies [7]. Therefore, we next carried out the selection among the other colonies. Fortunately, we found that colony #4, showing a rather high level of RL activity (2×10^6 U/1.6×10^5 cells), possessed a complete genome-length HCV-AH1 RNA without any deleted forms, although most of the other colonies possessed some amounts of a deleted form in addition to a complete genome-length HCV-AH1 RNA (data not shown). We demonstrated that the HCV RNA sequence was not integrated into the genomic DNA in colony #4 (data not shown). From these results, we finally selected colony #4, and it was thereafter referred to as AH1R and used for the following studies.

We first demonstrated that AH1R cells expressed sufficient levels of HCV proteins (Core, E2, and NS5B) by Western blot analysis for the evaluation of anti-HCV reagents, and the expression levels were almost equivalent to those in OR6 cells (Fig. 1b). In this analysis, we confirmed that the size of the E2 protein in AH1R cells was 7 kDa larger than that in OR6 cells (Fig. 1b), as observed previously [12]. This result indicates that AH1R cells express AH1 strain-derived E2 protein possessing two extra N-glycosylation sites [12]. We next demonstrated good correlations between the levels of RL activity and HCV RNA in AH1R cells (Fig. 1c), as we previously demonstrated in OR6 cells treated with IFN-α for 24 h [7]. These correlations indicate that AH1R cells were as useful as OR6 cells as a luciferase assay system.

Aa substitutions detected in genome-length HCV RNA in AH1R cells

To examine whether or not genome-length HCV RNA in AH1R cells possesses additional conserved mutations such as adaptive mutations, we performed a sequence analysis of HCV RNA in AH1R cells. The results (Fig. 2) revealed that

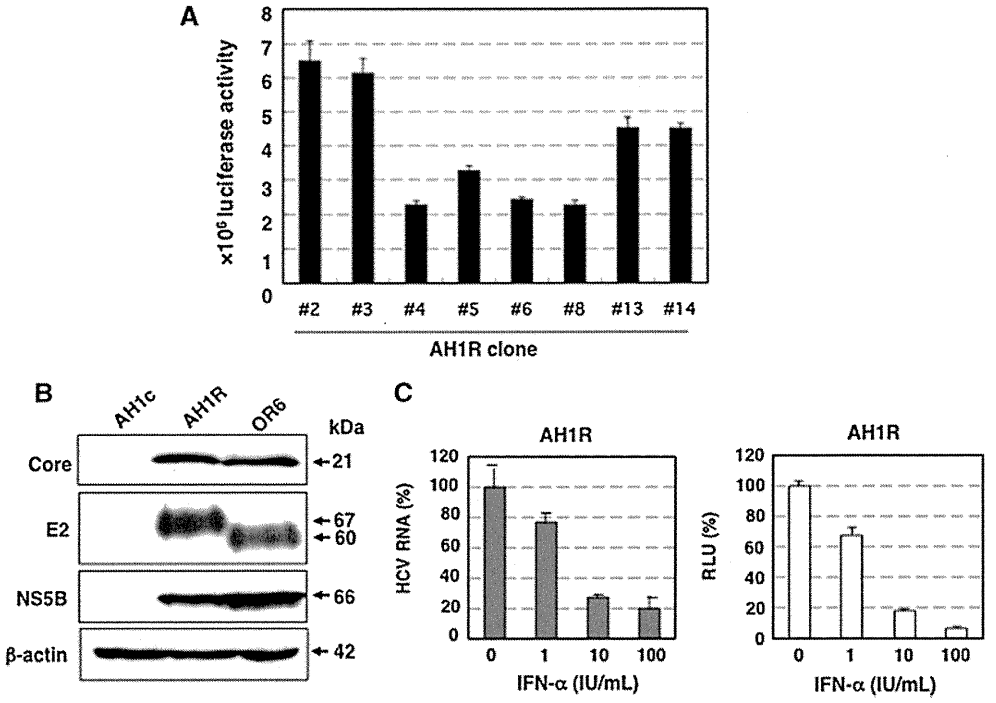

Fig. 1 Characterization of AH1R cells harboring genome-length HCV RNA. **a** Selection of G418-resistant cell clones. The levels of HCV RNA in G418-resistant cells were monitored by RL assay. **b** Western blot analysis. AH1c, AH1R, and OR6 cells were used for the comparison. *Core, E2,* and *NS5B* were detected by Western blot analysis. β-actin was used as a control for the amount of protein loaded per lane. **c** RL activity is correlated with HCV RNA level. The AH1R cells were treated with IFN-α (0, 1, 10, and 100 IU/mL) for 24 h, and then a luciferase reporter assay (*right panel*) and quantitative RT-PCR (*left panel*) were performed. The relative luciferase activity (RLU) (%) or HCV RNA (%) calculated at each point, when the level of luciferase activity or HCV RNA in non-treated cells was assigned to be 100%, is presented here

two additional mutations accompanying aa substitutions (W860R (NS2) and A1218E (NS3)) were detected commonly among the three independent clones sequenced, suggesting that these additional mutations are required for the efficient replication or stability of genome-length HCV RNA. The P1115L (NS3), L1262S (NS3), V1897A (NS4B), and V2360A (NS5A) mutations derived from the sAH1 replicon [12] were conserved in AH1R cell-derived clones. However, AH1-clone-2-specific mutations (T1338A and V1880A) were almost reverted to the consensus sequences of AH1 RNA [12] except for V1880A in AH1R clone 2 (Fig. 2). In addition, the Q63R (Core) mutation was observed in two of three clones (Fig. 2).

Comparison between the AH1R and OR6 assay systems regarding the sensitivities to IFN-α, IFN-γ, and CsA

Using quantitative RT-PCR analysis, we previously examined the anti-HCV activities of IFN-α, IFN-γ, and CsA in AH1 and O cells, and noticed different anti-HCV profiles of IFN-γ and CsA between AH1 and O cells [12]. In that study, AH1 cells seemed to be more sensitive than the O cells to CsA (significant difference was observed when 0.063, 0.12, or 0.25 μg/mL of CsA was used). Conversely, AH1 cells seemed to be less sensitive than the O cells to IFN-γ (significant difference was observed when 1 or 10 IU/mL of IFN-γ was used). However, we were not able to determine precisely the EC_{50} values of these reagents, because of the unevenness of the data obtained by RT-PCR.

After developing the AH1R assay system in this study, we determined the EC_{50} values of IFN-α, IFN-γ, and CsA using the AH1R assay and compared the values with those obtained by the OR6 assay. The results revealed that AH1R assay was more sensitive than OR6 assay to IFN-α (EC_{50}; 0.31 IU/mL for AH1R, 0.45 IU/mL for OR6) (Fig. 3a) and CsA (EC_{50}; 0.11 μg/mL for AH1R, 0.42 μg/mL for OR6) (Fig. 3b), and that the OR6 assay was more sensitive than the AH1R assay to IFN-γ (EC_{50}; 0.69 IU/mL for AH1R, 0.28 IU/mL for OR6) (Fig. 3c). Regarding these anti-HCV reagents, the anti-HCV activities observed between the AH1R and OR6 assays differed significantly in all of the concentrations examined (Fig. 3). In addition, regarding these anti-HCV reagents, cell growth was not suppressed within the concentrations used. Regarding IFN-γ and CsA, the present results clearly support those of our previous

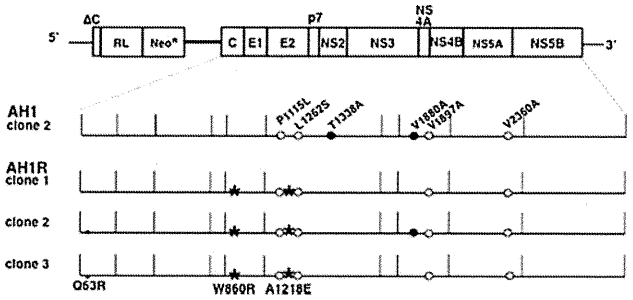

Fig. 2 Aa substitutions detected in intracellular AH1R genome-length HCV RNA. The *upper portion* shows schematic gene organization of genome-length HCV RNA encoding the *RL* gene developed in this study. Genome-length HCV RNA consists of 2 cistrons. In the first cistron, RL is translated as a fusion protein with Neo^R by HCV-IRES, and in the second cistron, all of HCV proteins (C-NS5B) are translated by encephalomyocarditis virus (EMCV)-IRES introduced in the region upstream of C-NS5B regions. Genome-length HCV RNA-replicating cells possess the G418-resistant phenotype because Neo^R is produced by the efficient replication of genome-length HCV RNA. Therefore, when genome-length HCV RNA is excluded from the cells or when its level is decreased, the cells are killed in the presence of G418. In this system, anti-HCV activity is able to evaluate the value of the reporter (RL activity) instead of the quantification of HCV RNA or HCV proteins. In addition, it has been known that the infectious HCV is not produced from this RNA replication system [3, 4, 6]. Core to NS5B regions of three independent clones (*AH1R clones 1–3*) sequenced are presented. W860R and A1218E conserved substitutions are indicated by *asterisks*. Q63R substitutions detected in two of three clones are each indicated by a *small dot*. Core to NS5B regions of *AH1 clone 2*, used to establish the AH1R cell line, are also presented. AH1-specific conserved substitutions and *AH1-clone-2*-specific substitutions are indicated by *open circles* and *black circles*, respectively

study [12]. Therefore, we suggest that the diverse effects of these anti-HCV reagents are due to the difference in HCV strains, although we are not able to completely exclude the possibility that AH1R cells are compromised cells causing the different responses against anti-HCV reagents. In summary, the previous and present findings suggest that the AH1R assay system is also useful for the evaluation of anti-HCV reagents as an independent assay system.

Anti-HCV activity of rolipram was clearly observed in the AH1R assay, but not in the OR6 assay

From the above findings, we supposed that the anti-HCV reagents reported to date might show diverse effects between the drug assay systems derived from the different HCV strains. To test this assumption, we used the AH1R and OR6 assay systems to evaluate the anti-HCV activity of more than 10 pre-existing drugs (6-Azauridine, bisindoly maleimide 1, carvedilol, cehalotaxine, clemizole, 2′-deoxy-5-fluorouridine, esomeprazole, guanazole, hemin, homoharringtonine, methotrexate, nitazoxanide, resveratrol, rolipram, silibinin A, Y27632, etc.), which other groups had evaluated using an assay system derived from the Con1 strain (genotype 1b) or JFH-1 strain (genotype 2a). The results revealed that most of these reagents in the AH1R assay showed similar levels of anti-HCV activities compared with those in the OR6 assay or those of the previous studies (data not shown). However, we found that only rolipram, a selective phosphodiesterase 4 (PDE4) inhibitor [16] that is used as an anti-inflammatory drug, showed moderate anti-HCV activity (EC_{50} 31 μM; $CC_{50} > 200$ μM; $SI > 6$) in the AH1R assay, but no such activity in the OR6 assay (upper panel in Fig. 4a). This remarkable difference was confirmed by Western blot analysis (lower panel in Fig. 4a). It is unlikely that rolipram's anti-HCV activity is due to the inhibition of exogenous RL, Neo^R or encephalomyocarditis virus internal ribosomal entry site (EMCV-IRES), all of which are encoded in the genome-length HCV RNA, because the AH1R and OR6 assay systems possess the same structure of genome-length HCV RNA except for HCV ORF. To demonstrate that rolipram's anti-HCV activity is not due to the clonal specificity of the cells or the specificity of genome-length HCV RNA, we examined the anti-HCV activity of rolipram using the monoclonal HCV replicon RNA-replicating cells (sAH1 cells for AH1 strain [12], and sO cells for O strain [13]). The results

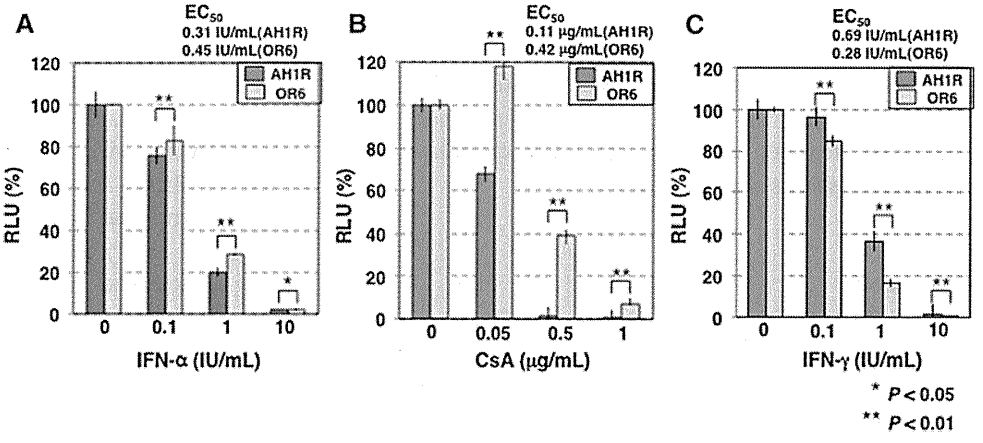

Fig. 3 The diverse effects of anti-HCV reagents on AH1R and OR6 assay systems. AH1R and OR6 cells were treated with anti-HCV reagents for 72 h, and then the RL assay was performed as described in Fig. 1c. **a** Effect of IFN-α. **b** Effect of CsA. **c** Effect of IFN-γ

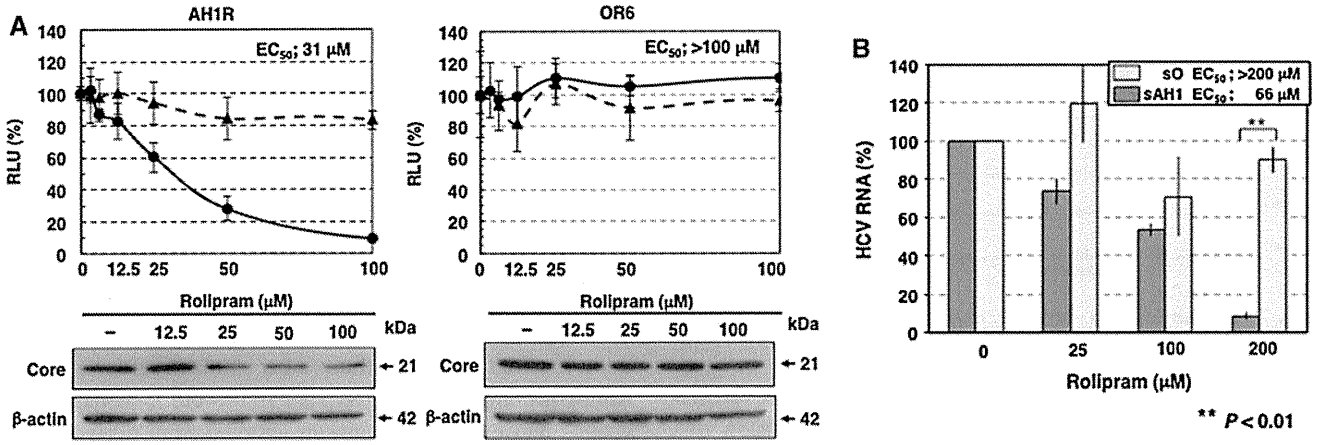

Fig. 4 Anti-HCV activity of rolipram. **a** Rolipram sensitivities on genome-length HCV RNA replication in AH1R and OR6 assay systems. AH1R and OR6 cells were treated with rolipram for 72 h, followed by RL assay (*black circle* with *linear line* in the *upper panels*) and WST-1 assay (*black triangle* with *broken line* in the *upper panels*). The relative value (%) calculated at each point, when the level in non-treated cells was assigned to 100%, is presented here. Western blot analysis of the treated cells for the HCV Core was also performed (*lower panels*). **b** Rolipram sensitivities on HCV replicon RNA replication in sAH1 and sO cells. sAH1 and sO cells were treated with rolipram for 72 h, and extracted total RNAs were subjected to quantitative RT-PCR for HCV 5′ untranslated region as described previously [7]. The HCV RNA (%) calculated at each point, when the level of HCV RNA in non-treated cells was assigned to be 100%, is presented here

revealed by quantitative RT-PCR that rolipram showed moderate anti-HCV activity (EC_{50} 66 μM) in sAH1 cells, but no such activity in sO cells (Fig. 4b). Anti-HCV activity of rolipram in sAH1 cells was a little weaker than that in AH1R cells (Fig. 4b). The similar phenomenon that the anti-HCV activity in genome-length HCV RNA-based reporter assay is stronger than that in HCV subgenomic replicon-based reporter assay was observed regarding other anti-HCV reagents in our previous studies [14, 17, 18]. This result suggests that the anti-HCV activity of rolipram is not either a clone-specific or genome-length HCV RNA-specific phenomenon. In our previous studies also [14, 18], we demonstrated that anti-HCV activities of several reagents including ribavirin and statins were not due to the clonal specificity of the cells. On the other hand, it was recently reported that rolipram did not show anti-HCV activity in the JFH-1 strain-derived assay [19]. Taken together, the previous and present results suggest that rolipram's anti-HCV activity differs depending on the HCV strain. In summary, rolipram was identified as a new anti-HCV candidate using the AH1R assay system.

Discussion

In the present study, we developed for the first time a drug assay system (AH1R), derived from the HCV-AH1 strain (from a patient with acute hepatitis C), in which HCV-AH1 RNA is efficiently replicated. Using this system, we found that rolipram, an anti-inflammatory drug, had potential anti-HCV activity. This potential had not been detected by preexisting assay systems such as OR6, in which HCV-O RNA was derived from an HCV-positive blood donor. Since an HCV replicon harboring the sAH1 cell line, the parent of the AH1R cell line, was obtained from OR6-cured cells [12], the divergence in rolipram's effects between AH1R and OR6 cells is probably attributable to the difference in HCV strains rather than to the difference in cell clones. Indeed, rolipram's anti-HCV activity was not observed in another ORL8 assay system (O strain), which was recently developed using a new hepatoma Li23 cell line (data not shown) [15]. Therefore, we propose that multiple assay systems derived from different HCV strains are required for the discovery of anti-HCV reagents such as rolipram or for the objective evaluation of anti-HCV activity.

Comparative evaluation analysis of anti-HCV activities of IFN-α, IFN-γ, and CsA using AH1-strain-derived AH1R and O-strain-derived OR6 assay systems demonstrated that each of these anti-HCV reagents showed significantly diverse antiviral effects between the two systems. Regarding IFN-γ and CsA, the present results obtained using a luciferase reporter assay fully supported our previous findings [12] using quantitative RT-PCR analysis. However, in the present analysis, we noticed that IFN-α also showed significantly diverse effects (especially at less than 1 IU/mL) between the AH1R and OR6 assays.

The differences in IFN-α sensitivity may be attributable to the difference in aa sequences in the IFN sensitivity-determining region (ISDR; aa 2209-2248 in the HCV-1b genotype), in which aa substitutions correlate well with IFN sensitivity in patients with chronic hepatitis C [20], because the AH1 strain possesses three aa substitutions (T2217A, H2218R, and A2224 V) in ISDR, whereas the O strain possesses no aa substitutions. However, no report has demonstrated the correlation between IFN sensitivity and the substitution numbers in ISDR using the cell culture-based HCV RNA replication system.

Alternatively, Akuta et al. [21] reported that aa substitutions at position 70 and/or position 91 in the HCV Core region of patients infected with the HCV-1b genotype are pretreatment predictors of null virological response (NVR) to pegylated IFN/ribavirin combination therapy. In particular, substitutions of arginine (R) by glutamine (Q) at position 70, and/or leucine (L) by methionine (M) at position 91, were common in NVR. The patients with position-70 substitutions often showed little or no decrease in HCV RNA levels during the early phase of IFN-α treatment [21]. Regarding this point, it is interesting that position 70 in the AH1 strain is R (wild type) and that in the O strain is Q (mutant type), whereas position 91 is L (wild type) in both strains. Therefore, wild-type R in position 70 of the AH1 strain may contribute to the high sensitivity to IFN-α in the AH1R assay. Regarding positions 70 and 91 of the HCV Core, it is noteworthy that, among all of the HCV strains used thus far to develop HCV replicon systems, only the AH1 strain possesses double wild-type aa (data not shown). Therefore, the AH1R assay system may be useful for further study of sensitivity to IFN/ribavirin treatment.

The anti-HCV activity of rolipram, which is currently used as an anti-inflammatory drug, is interesting, although its anti-HCV mechanism is unclear. As a selective PDE4 inhibitor [16], rolipram may attenuate fibroblast activities that can lead to fibrosis and may be particularly effective in the presence of transforming growth factor (TGF)-β1-induced fibroblast stimulation [22]. On the other hand, HCV enhances hepatic fibrosis progression through the generation of reactive oxygen species and the induction of TGF-β1 [23]. Taken together, the previous and present results suggest that rolipram may inhibit both HCV RNA replication and HCV-enhanced hepatic fibrosis. However, it is unclear that rolipram shows anti-HCV activity against the majority of HCV strains, because rolipram has been effective for AH1 strain, but not for O strain. Although rolipram's anti-HCV activity would be HCV-strain-specific, it is not clear which HCV strain is the major type regarding the sensitivity to rolipram. Since developed assay systems using genome-length HCV RNA-replicating cells are limited to several HCV strains including O and AH1 strains to date, further analysis using the assay systems of other HCV strains will be needed to clarify this point.

In this study, we demonstrated that the AH1R assay system, which was for the first time developed using an HCV strain derived from a patient with acute hepatitis C, showed different sensitivities against anti-HCV reagents in comparison with assay systems in current use, such as OR6 assay. Therefore, AH1R assay system would be useful for various HCV studies including the evaluation of anti-HCV reagents and the identification of antiviral targets.

Acknowledgment This study was supported by grants-in-aid for research on hepatitis from the Ministry of Health, Labor, and Welfare of Japan. K. M. was supported by a Research Fellowship for Young Scientists from the Japan Society for the Promotion of Science.

References

1. N. Kato, Acta Med. Okayama **55**, 133–159 (2001)
2. N. Kato, M. Hijikata, Y. Ootsuyama, M. Nakagawa, S. Ohkoshi, T. Sugimura, K. Shimotohno, Proc. Natl. Acad. Sci. USA **87**, 9524–9528 (1990)
3. R. Bartenschlager, S. Sparacio, Virus Res. **127**, 195–207 (2007)
4. D. Moradpour, F. Penin, C.M. Rice, Nat. Rev. Microbiol. **5**, 453–463 (2007)
5. V. Lohmann, F. Korner, J. Koch, U. Herian, L. Theilmann, R. Bartenschlager, Science **285**, 110–113 (1999)
6. M. Ikeda, N. Kato, Adv. Drug Deliv. Rev. **59**, 1277–1289 (2007)
7. M. Ikeda, K. Abe, H. Dansako, T. Nakamura, K. Naka, N. Kato, Biochem. Biophys. Res. Commun. **329**, 1350–1359 (2005)
8. K. Naka, M. Ikeda, K. Abe, H. Dansako, N. Kato, Biochem. Biophys. Res. Commun. **330**, 871–879 (2005)
9. M. Ikeda, K. Abe, M. Yamada, H. Dansako, K. Naka, N. Kato, Hepatology **44**, 117–125 (2006)
10. A. Nozaki, M. Morimoto, M. Kondo, T. Oshima, K. Numata, S. Fujisawa, T. Kaneko, E. Miyajima, S. Morita, K. Mori, M. Ikeda, N. Kato, K. Tanaka, Arch. Virol. **155**, 601–605 (2010)
11. M. Ikeda, Y. Kawai, K. Mori, M. Yano, K. Abe, G. Nishimura, H. Dansako, Y. Ariumi, T. Wakita, K. Yamamoto, N. Kato, Liver Int. **31**, 871–880 (2011)
12. K. Mori, K. Abe, H. Dansako, Y. Ariumi, M. Ikeda, N. Kato, Biochem. Biophys. Res. Commun. **371**, 104–109 (2008)
13. N. Kato, K. Sugiyama, K. Namba, H. Dansako, T. Nakamura, M. Takami, K. Naka, A. Nozaki, K. Shimotohno, Biochem. Biophys. Res. Commun. **306**, 756–766 (2003)
14. K. Mori, M. Ikeda, Y. Ariumi, H. Dansako, T. Wakita, N. Kato, Virus Res. **157**, 61–70 (2011)
15. N. Kato, K. Mori, K. Abe, H. Dansako, M. Kuroki, Y. Ariumi, T. Wakita, M. Ikeda, Virus Res. **146**, 41–50 (2009)
16. S.J. MacKenzie, M.D. Houslay, Biochem. J. **347**, 571–578 (2000)
17. M. Yano, M. Ikeda, K. Abe, H. Dansako, S. Ohkoshi, Y. Aoyagi, N. Kato, Antimicrob. Agents Chemother. **51**, 2016–2027 (2007)
18. G. Nishimura, M. Ikeda, K. Mori, T. Nakazawa, Y. Ariumi, H. Dansako, N. Kato, Antiviral Res. **82**, 42–50 (2009)
19. P. Gastaminza, C. Whitten-Baue, F.V. Chisari, Proc. Natl. Acad. Sci. USA **107**, 291–296 (2010)
20. N. Enomoto, I. Sakuma, Y. Asahina, M. Kurosaki, T. Murakami, C. Yamamoto, Y. Ogura, N. Izumi, F. Marumo, C. Sato, N. Engl. J. Med. **334**, 77–81 (1996)

21. N. Akuta, F. Suzuki, Y. Kawamura, H. Yatsuji, H. Sezaki, Y. Suzuki, T. Hosaka, M. Kobayashi, M. Kobayashi, Y. Arase, K. Ikeda, H. Kumada, J. Med. Virol. **79**, 1686–1695 (2007)
22. S. Togo, X. Liu, X. Wang, Am. J. Physiol. Lung Cell. Mol. Physiol. **296**, L959–L969 (2009)
23. W. Lin, W.L. Tsai, R.X. Shao, G. Wu, L.F. Peng, L.L. Barlow, W.J. Chung, L. Zhang, H. Zhao, J.Y. Jang, R.T. Chung, Gastroenterology **138**, 2509–2518 (2010)

THE JOURNAL OF BIOLOGICAL CHEMISTRY VOL. 286, NO. 43, pp. 37264–37273, October 28, 2011

Role of the Endoplasmic Reticulum-associated Degradation (ERAD) Pathway in Degradation of Hepatitis C Virus Envelope Proteins and Production of Virus Particles*[S]

Received for publication, May 7, 2011, and in revised form, August 18, 2011 Published, JBC Papers in Press, August 30, 2011, DOI 10.1074/jbc.M111.259085

Mohsan Saeed[§], Ryosuke Suzuki[‡], Noriyuki Watanabe[‡], Takahiro Masaki[‡], Mitsunori Tomonaga[‡], Amir Muhammad[¶], Takanobu Kato[‡], Yoshiharu Matsuura[‖], Haruo Watanabe[§], Takaji Wakita[‡], and Tetsuro Suzuki[‡‡1]**

*From the [‡]Department of Virology II, National Institute of Infectious Diseases, Tokyo 162-8640, Japan, the [§]Department of Infection and Pathology, Graduate School of Medicine, the University of Tokyo, Tokyo 113-0033, Japan, the [¶]Department of Pathology, Khyber Girls Medical College, Peshawar 25000, Pakistan, the [‖]Research Institute of Microbial Diseases, Osaka University, Osaka 565-0871, Japan, the **National Institute of Infectious Diseases, Tokyo 162-8640, Japan, and the [‡‡]Department of Infectious Diseases, Hamamatsu University School of Medicine, Hamamatsu 431-3192, Japan*

Background: HCV causes ER stress in the infected cells.
Results: HCV-induced ER stress leads to increased expression of certain proteins that in turn enhance the degradation of HCV glycoproteins and decrease production of virus particles.
Conclusion: HCV infection activates the ERAD pathway, leading to modulation of virus production.
Significance: ERAD plays a crucial role in the viral life cycle.

Viral infections frequently cause endoplasmic reticulum (ER) stress in host cells leading to stimulation of the ER-associated degradation (ERAD) pathway, which subsequently targets unassembled glycoproteins for ubiquitylation and proteasomal degradation. However, the role of the ERAD pathway in the viral life cycle is poorly defined. In this paper, we demonstrate that hepatitis C virus (HCV) infection activates the ERAD pathway, which in turn controls the fate of viral glycoproteins and modulates virus production. ERAD proteins, such as EDEM1 and EDEM3, were found to increase ubiquitylation of HCV envelope proteins via direct physical interaction. Knocking down of EDEM1 and EDEM3 increased the half-life of HCV E2, as well as virus production, whereas exogenous expression of these proteins reduced the production of infectious virus particles. Further investigation revealed that only EDEM1 and EDEM3 bind with SEL1L, an ER membrane adaptor protein involved in translocation of ERAD substrates from the ER to the cytoplasm. When HCV-infected cells were treated with kifunensine, a potent inhibitor of the ERAD pathway, the half-life of HCV E2 increased and so did virus production. Kifunensine inhibited the binding of EDEM1 and EDEM3 with SEL1L, thus blocking the ubiquitylation of HCV E2 protein. Chemical inhibition of the ERAD pathway neither affected production of the Japanese encephalitis virus (JEV) nor stability of the JEV envelope protein. A co-immunoprecipitation assay showed that EDEM orthologs do not bind with JEV envelope protein. These findings highlight the crucial role of the ERAD pathway in the life cycle of specific viruses.

Quality control of proteins, such as the elimination of misfolded proteins, is largely connected with the endoplasmic reticulum (ER),[2] which is an organelle responsible for the folding and distribution of secretory proteins to their sites of action. This pathway is termed ER-associated degradation (ERAD) and is triggered by ER stress. It results in retrotranslocation of misfolded proteins into the cytosol, followed by polyubiquitylation and proteasomal degradation (1). Several viral infections have been reported to trigger the ERAD pathway (2–4); however, the role of this pathway in the life cycle of viruses remains poorly defined.

Initiation of the ERAD pathway occurs from the oligomerization and autophosphorylation of IRE1, an ER stress sensor. The activated IRE1 removes an intron from X-box-binding protein 1 (XBP1) mRNA, which then encodes a potent transcription factor for activation of genes, for example, ER degradation-enhancing α-mannosidase-like protein (EDEM). EDEM1 (5), along with its two homologs EDEM2 (6) and EDEM3 (7), as well as ER mannosidase I (ER ManI), belong to the glycoside hydrolase 47 family. EDEMs are thought to function as lectins that deliver misfolded glycoproteins to the ERAD pathway. However, the precise mechanism by which they assist in glycoprotein quality control remains unclear.

Hepatitis C virus (HCV) infection is a major cause of chronic liver disease. The RNA genome of HCV, a member of the Fla-

* This work was supported by grants-in-aid from the Ministry of Health, Labor and Welfare, and from the Ministry of Education, Culture, Sports, Science, and Technology, Japan.
[S] The on-line version of this article (available at http://www.jbc.org) contains supplemental Figs. S1–S7.
[1] To whom correspondence should be addressed: Dept. of Infectious Diseases, Hamamatsu University School of Medicine, Hamamatsu 431-3192, Japan. Tel.: 81-53-435-2336; Fax: 81-53-435-2338; E-mail: tesuzuki@hama-med.ac.jp.

[2] The abbreviations used are: ER, endoplasmic reticulum; CHX, cycloheximide; EDEM, ER degradation-enhancing α-mannosidase-like protein; ERAD, ER-associated degradation; HCV, hepatitis C virus; JEV, Japanese encephalitis virus; KIF, kifunensine; ManI, mannosidase I; m.o.i., multiplicity of infection; TM, tunicamycin; XBP1, X-box-binding protein 1; IRE, inositol-requiring enzyme.

viviridae family, encodes the viral structural proteins Core, E1, E2, and p7, as well as six nonstructural proteins (8, 9). Two *N*-glycosylated envelope proteins E1 and E2 are exposed on the surface of the virus and are necessary for viral entry.

The aim of this study was to investigate whether the ERAD pathway is activated upon HCV infection and whether this affects the quality control of virus glycoproteins and virion production. We show that HCV infection triggers the ERAD pathway, possibly through IRE1-mediated splicing of XBP1. Moreover, EDEM1 and EDEM3, but not EDEM2, interact with HCV glycoproteins, resulting in increased ubiquitylation. EDEM1 knockdown and chemical inhibition of the ERAD pathway increases glycoprotein stability, as well as production of infectious virus particles, whereas overexpression of EDEM1 decreases virion production. These results provide insight into the mechanism by which HCV triggers the ERAD pathway and subsequently affects the quality control of virus glycoproteins and virus particle production.

EXPERIMENTAL PROCEDURES

Cell Culture and Chemicals—Human hepatoma cells HuH-7 and HuH-7.5.1 (a gift from Dr. F. V. Chisari (The Scripps Research Institute) (10) and human embryonic kidney cells 293T were cultured at 37 °C and 5% CO_2 in DMEM containing 10% FBS, 10 mM HEPES, 1 mM sodium pyruvate, nonessential minimum amino acids, 100 units/ml penicillin, and 100 μg/ml streptomycin. Tunicamycin (TM) was purchased from Sigma-Aldrich, and kifunensine (KIF) was purchased from Toronto Research Chemicals (Ontario, Canada).

Preparation of Virus Stock—HCV JFH-1 was generated by introducing *in vitro* transcribed RNA into HuH-7.5.1 cells by electroporation, and virus stocks were prepared by infecting at a multiplicity of infection (m.o.i.) of 0.01, as described previously (10). Infected cells were grown in culture medium containing 2% FBS, and supernatants were collected after multiple passages to get high titer virus. The supernatants were concentrated using a 500-kDa hollow fiber module (GE Healthcare) resulting in ~90% recovery of the virus. Focus-forming units were measured with an anti-HCV core antibody to determine virus titration (2H9, described below). Virus stocks containing 1×10^7 focus-forming units/ml were divided into small aliquots and stored at −80 °C until use. rAT strain of Japanese encephalitis virus (JEV) (11) was used to generate virus stock.

Plasmids—cDNAs of mouse EDEM1-HA, EDEM2, and EDEM3-HA, having 92, 93, and 91% amino acid homology with their human orthologs, respectively, were a kind gift from Drs. N. Hosokawa (Kyoto University) and K. Nagata (Kyoto Sangyo University). A HA tag was attached to the C terminus of EDEM2 by PCR, and sequencing analysis was performed to confirm the sequence. To generate pJFH/E1dTM-myc and pJFH/E2dTM-myc, HCV E1 encoding amino acids 170–352 and HCV E2 encoding amino acids 340–714 of JFH-1 polyprotein were amplified by PCR with forward primer and reverse primer containing NotI and XbaI restriction sites, respectively, and cloned into a NotI/XbaI site of the pEF1/Myc-His plasmid (Invitrogen). The pCAGC105E plasmid carrying PrM and E proteins of the rAT strain of JEV has been described (12). Plasmids carrying the firefly luciferase reporter gene under control of the intact promoter of GRP78 and GRP94 or the defective promoter lacking ERSE elements have been described (13) and were a kind gift from Dr. K. Mori (Kyoto University).

Antibodies—Rabbit polyclonal antibodies included anti-HA (Sigma-Aldrich), anti-HCV NS5A (14), anti-SEL1L (Sigma-Aldrich), anti-ubiquitin (MBL, Nagoya, Japan), and anti-JEV E antibodies. The mouse monoclonal antibodies were anti-HA (clone 16B12; Covance, Emeryville, CA), anti-HCV E2 (clone 8D10-3),[3] anti-β-actin (clone AC15; Sigma-Aldrich), anti-HCV core (clone 2H9) (15), and anti-Myc (clone 9E10; Santa Cruz Biotechnology, Santa Cruz, CA) antibodies. Anti-JEV antibodies have been described (16) and were a kind gift from Drs. C. K. Lim and T. Takasaki (National Institute of Infectious Diseases).

Analysis of XBP1 Splicing—Total RNA was extracted from cells using Isogen (Nippon Gene, Tokyo, Japan) following the manufacturer's protocol, and 2 μg of RNA was subjected to cDNA synthesis using oligo(dT) and Superscript III (Invitrogen). PCR was carried out using specific primers 5′-AAACAGAGTAGCAGCTCAGACTGC-3′ and 5′-GTATCTCTAAGACTAGGGGCTTGGTA-3′ for XBP1 and 5′-TCCTGTGGCATCCACGAAACT-3′ and 5′-GAAGCATTTGCGGTGGACGAT-3′ for β-actin to generate PCR fragments of 598 bp for unspliced XBP1, 572 bp for spliced XBP1, and 315 bp for β-actin. The following cycling conditions were used to amplify the genes: 1 cycle of 98 °C for 3 min, followed by 30 cycles of 98 °C for 20 s, 55 °C for 30 s, and 72 °C for 1 min, followed by a final extension of 72 °C for 10 min. The PCR product of XBP1 was further digested with PstI enzyme (New England Biolabs) and resolved on a 2% agarose gel prepared in TAE buffer. Unspliced XBP1 yielded two smaller fragments of 291 and 307 bp whereas spliced XBP1 stayed intact due to loss of the restriction site after splicing.

Gene Microarray Analysis—For microarray analysis, RNA was extracted from HuH-7.5.1 cells at 48 and 72 h after JFH-1 infection. Cells treated for 12 h with 5 μg/ml TM served as a positive control. Hybridization was performed on a 3D-Gene (see 3D-Gene web site) Human Oligonucleotide chip 25k (Toray Industries Inc., Tokyo, Japan). For efficient hybridization, this microarray chip has three dimensions and is constructed with a well between the probes and cylinder stems with 70-mer oligonucleotide probes on the top. Total RNA was labeled with Cy3 or Cy5 using the Amino Allyl MessageAMP II aRNA Amplification kit (Applied Biosystems). The Cy3- or Cy5-labeled aRNA pools were subjected to hybridization for 16 h using the supplier's protocol. Hybridization signals were scanned using a ScanArray Express Scanner (PerkinElmer Life Sciences) and processed by GenePixPro version 5.0 (Molecular Devices, Sunnyvale, CA). Detected signals for each gene were normalized using a global normalization method (Cy3/Cy5 ratio median = 1). Genes with Cy3/Cy5 normalized ratios $>\log_2 1.0$ or $<\log_2 \_1.0$ were defined, respectively, as significantly up- or down-regulated genes.

Quantification of Cellular Gene Expression—Gene expression levels were measured using predesigned assay-on-demand (Applied Biosystems). RT-PCR amplification was performed

[3] D. Akazawa, N. Nakamura, and T. Wakita, unpublished data.

under the following conditions: 48 °C for 30 min, 95 °C for 10 min, 50 cycles of 95 °C for 15 s, and 60 °C for 1 min. Standard curves were constructed on a 1:5 serial dilution of the RNA template. The results were normalized to GAPDH mRNA levels.

Determination of Protein Stability—HuH-7 cells were infected with HCV JFH-1 at a m.o.i. of 2. Six hours after infection, the cells were either treated with KIF or transfected with EDEM1 siRNA. Forty hours later, culture medium was replaced with 100 μg/ml cycloheximide (CHX). Cells, including floating cells, were harvested at different time points after CHX addition, and immunoblotting was performed to determine the amount of HCV E2.

Plasmid Transfection and Immunoprecipitation—HuH-7 or 293T cells were seeded in 6-well cell culture plates at 3×10^5 cells/well and cultured overnight. Plasmid DNA was transfected into cells using TranIT-LT1 transfection reagent (Mirus, Madison, WI). Cells were harvested at 48 h after transfection, washed once with 1 ml of PBS, and lysed in 200 μl of lysis buffer (20 mM Tris-HCl, pH 7.4, 135 mM NaCl, 1% Triton X-100, and 10% glycerol supplemented with 50 mM NaF, 5 mM Na_3VO_4, and protease inhibitor mixture tablets (Roche Diagnostics). Cell lysates were sonicated at 4 °C for 10 min, incubated for 30 min at 4 °C, and centrifuged at 14,000 × *g* for 5 min at 4 °C. After preclearing for 2 h, the supernatants were immunoprecipitated overnight by rotating with 1.5 μl of anti-HA monoclonal antibody (16B12) or anti-HCV E2 monoclonal antibody (clone 8D10-3) at 4 °C. The immunocomplexes were then captured on protein G-agarose beads (Invitrogen) by rotation-incubation at 4 °C for 3 h. Beads were subsequently precipitated by centrifugation at 800 × *g* for 1 min and washed five times with lysis buffer. Finally, proteins bound to the beads were boiled in 40 μl of SDS sample buffer and subjected to SDS-PAGE.

Western Blotting—Proteins resolved by SDS-PAGE were transferred onto PVDF membranes (Immobilon; Millipore). After blocking in 2% skim milk, the membranes were probed with primary antibodies followed by exposure to peroxidase-conjugated secondary antibodies and visualization with an ECL Plus Western blotting detection system (GE Healthcare). The intensity of the bands was measured using a computerized imaging system (ImageJ software; National Institutes of Health).

Small Interfering RNA (siRNA) Transfection—HuH-7 cells were transfected with duplex siRNAs at a final concentration of 10 nM using Lipofectamine RNAiMAX (Invitrogen). Three siRNAs for each gene were examined for knock-down efficiency and cytotoxic effects. The siRNA with best performance was selected for further experiments. Target sequences of the siRNAs which exhibited the best knock-down efficiencies were as follows: EDEM1 (sense) 5′-CAUAUCCUCGGGUGAAUCUtt-3′, EDEM2 (sense) 5′-GAAUGUCUCAGAAUUCCAAtt-3′, EDEM3 (sense) 5′-CAUGAGACUACAAAUCUUAtt-3′, IRE1 (sense) 5′-GGACGUGAGCGACAGAAUAtt-3′. 5′-GGUGUCCUUACCAUACUAAtt-3′ served as a negative control. The lowercase letters denote overhanging deoxyribonucleotides.

Quantification of HCV Core and RNA—HCV core was quantified using an enzyme immunoassay (Ortho HCV antigen ELISA kit; Ortho Clinical Diagnostics, Tokyo, Japan). HCV RNA was quantified as described (17).

Statistical Analysis—Student's *t* test was employed to calculate the statistical significance of the results. $p < 0.05$ was considered significant.

RESULTS

HCV Infection Induces XBP1 mRNA Splicing and EDEM Expression—XBP1 plays a key role in activating the ERAD pathway, which mediates unfolded protein response in the ER. Under conditions of ER stress, XBP1 mRNA is processed by unconventional splicing and translated into functional XBP1, which in turn mediates transcriptional up-regulation of a variety of ER stress-dependent genes. The resultant activation of downstream pathways boosts the efficiency of ERAD, which coincides with elevated transcription of EDEMs. To validate our method for detecting activation of the ERAD pathway, we exposed HuH-7.5.1 cells to TM, which is a typical ER stress inducer, and performed an assay to quantify spliced XBP1 mRNA, as described under "Experimental Procedures," at different time points after treatment. The spliced form of XBP1 mRNA started accumulating within these cells as early as 2 h after exposure to TM (Fig. 1*A*), and levels remained elevated until at least 12 h after treatment. Quantitative RT-PCR showed that mRNA levels of EDEM1, EDEM2, and EDEM3 were elevated in TM-treated cells whereas ER ManI, which is not an ER stress-responsive gene, did not show any up-regulation (Fig. 1*B*). To examine involvement of the ERAD pathway in the HCV life cycle, we infected HuH-7.5.1 cells with JFH-1 at m.o.i. of 5 and analyzed XBP1 mRNA splicing and EDEM up-regulation. Upon infection, the fragment corresponding to spliced XBP1 mRNA, was detectable 8 h after infection, and the difference in splicing between mock- and HCV-infected cells became more pronounced at 48 h after infection and then persisted (Fig. 1*C*). Increased levels of XBP1 mRNA splicing were dependent on the m.o.i. (supplemental Fig. 1*A*), suggesting that expression of active XBP1 was induced by HCV infection. A small amount of spliced XBP1 was detected in mock-infected cells, presumably because of some intrinsic stress. A 3.1-fold increase in the level of EDEM1 mRNA was observed at 3–4 days after infection ($p < 0.05$). Increases in EDEM2 and EDEM3 mRNA levels were moderate and reached ~1.5-fold, whereas ER ManI mRNA exhibited no change after infection (Fig. 1*D*). Expression of EDEMs, particularly EDEM1, was up-regulated in accordance with HCV infection titers (supplemental Fig. 1*B*). Knocking down the IRE1 gene (Fig. 1*E*) effectively reversed the accumulation of spliced XBP1, as well as the transcriptional up-regulation of EDEM1 (Fig. 1*F*), thus confirming that HCV infection induces ERAD through the IRE1-XBP1 pathway.

To enable a comprehensive investigation of the transcriptional changes that occur, up- and down-regulation of the transcriptome was examined in HCV-infected cells and in TM-treated cells. The results were compared with those of mock-transfected cells at each time point. A range of genes involved in ER stress was found to be regulated in HCV-infected and in TM-treated cells (Fig. 2*A*). EDEM1 was signifi-

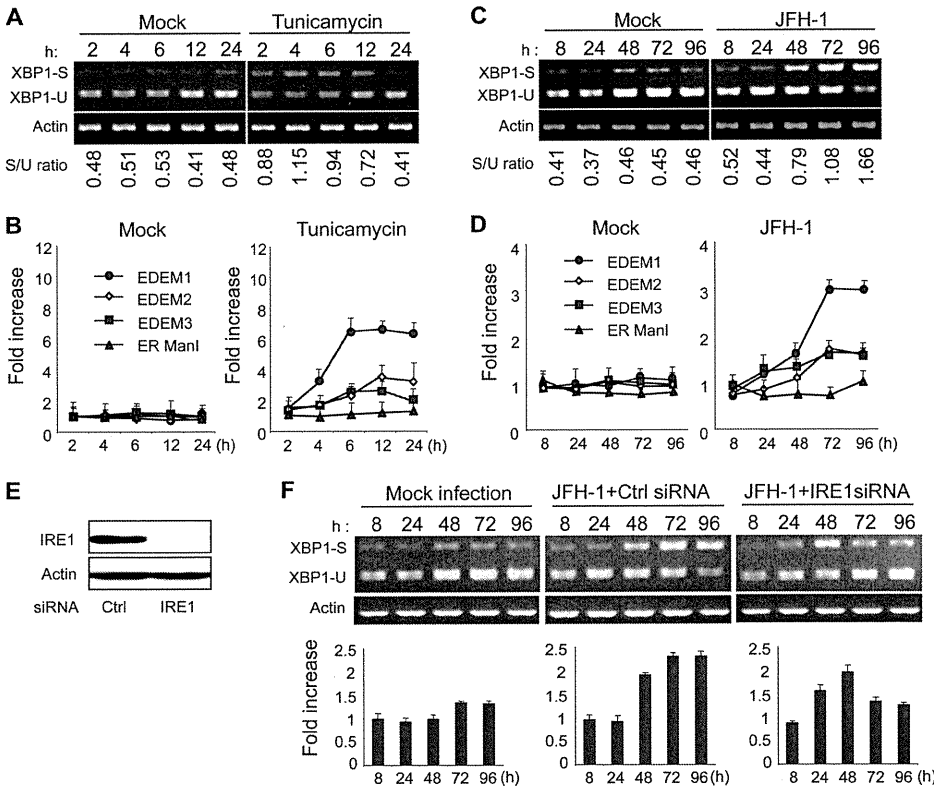

FIGURE 1. **Splicing of XBP1 mRNA and induction of ERAD gene expression in HCV JFH-1-infected cells.** *A*, splicing of XBP1 mRNA analyzed in mock- and TM (5 μg/ml)-treated HuH-7.5.1 cells at different time points after treatment. The *upper* and *lower bands* represent spliced and unspliced RNA, respectively. The *numbers* at the *bottom* of the *panel* indicate the density ratios of bands corresponding to spliced and unspliced XBP1. *B*, graphs showing the -fold induction of EDEM1, EDEM2, EDEM3, and ER Man1 mRNA in HuH-7.5.1 cells treated or untreated with TM. Data are normalized to GAPDH expression levels. The mean ± S.D. (*error bars*) of three independent experiments are shown. *C*, splicing of XBP1 mRNA analyzed in mock- and HCV JFH-1-infected HuH-7.5.1 cells (m.o.i. 5) at different time points after infection. *Numbers* at the *bottom* of the *panel* indicate the density ratios of bands corresponding to spliced and unspliced XBP1. *D*, real-time PCR analysis of EDEM1, EDEM2, EDEM3, and ER ManI mRNA induction in mock- and HCV-infected cells. Data are normalized to GAPDH expression. The mean ± S.D. of three independent experiments are shown. Note that a reduction in the level of GAPDH mRNA within infected cells was not observed until 96 h after infection when a slight decrease was observed. This led us to use GAPDH as a housekeeping gene in our experiments. *E*, Western blotting of IRE1 in cells transfected with mock or gene-specific siRNA of IRE1. *F*, splicing of XBP1 mRNA and induction of EDEM1 in HCV-infected cells after knocking down of the IRE1 gene. HuH-7.5.1 cells infected with JFH-1 at a m.o.i. of 5 were transfected with mock (*center*) or IRE1-specific siRNA (*right*) 48 h after infection, after which splicing of XBP1 (*upper*) and transcriptional up-regulation of EDEM1 (*lower*) were examined at the indicated time points after infection. The mean ± S.D. of two independent experiments are shown.

cantly up-regulated upon HCV infection, whereas expression levels of EDEM2 and EDEM3 remained unchanged. Although transcriptional changes caused by HCV infection in many of the genes listed are analogous to those that occur in cells treated with TM, up-regulation of two ER chaperone proteins, GRP78 and GRP94, was induced by TM treatment but not by HCV infection. This differential induction was confirmed by a reporter assay for GRP78 promoter and GRP94 promoter activities (Fig. 2*B*). These results are in agreement with a previously described finding that GRP78 and GRP94 are not responsive to HCV infection in hepatoma cells (18). It remains likely that HCV infection interferes with transcriptional activation of some ER chaperone proteins; however, the mechanism by which this occurs remains to be elucidated.

EDEMs Cause Ubiquitylation of HCV Glycoproteins and Enhance Their Degradation—Because EDEMs have been reported to enhance proteasomal degradation of ERAD substrates through direct binding, we investigated the interaction of EDEMs with HCV glycoproteins in 293T cells by co-transfecting the expression plasmids for E1dTM or E2dTM together with plasmids carrying either EDEM or ER ManI genes. Immunoprecipitation and immunoblotting demonstrated that each EDEM, but not ER ManI, was capable of interacting with E2 (Fig. 3*A*) and E1 (supplemental Fig. S2). HCV glycoproteins displayed enhanced mobility when co-expressed with EDEM1, EDEM3, or ER ManI, which could be due to the mannosidase activity of these proteins, which is lacking in EDEM2 (6). HCV primarily replicates in hepatocytes so we examined the interaction of EDEMs with E2dTM in HuH-7 cells as well, which yielded similar results (data not shown). E2dTM lacks the transmembrane domain, which could affect its folding and ER retention and thus modulate the ability of this protein to interact with EDEMs and ER ManI. Second, E1 and E2 glycoproteins assemble as noncovalent heterodimers to make functional complexes, which may alter the interaction of these proteins with EDEMs. To address these issues, we co-transfected HuH-7 cells with plasmids carrying full-length E1E2 glycoproteins together with plasmids carrying either EDEMs or ER ManI. Similar phenotypes were produced following transfection full-length E1E2 proteins (supplemental Fig. S3*A*), demonstrating that functional complexes of HCV glycoproteins bind with EDEMs. Recently, we have reported on the development of a

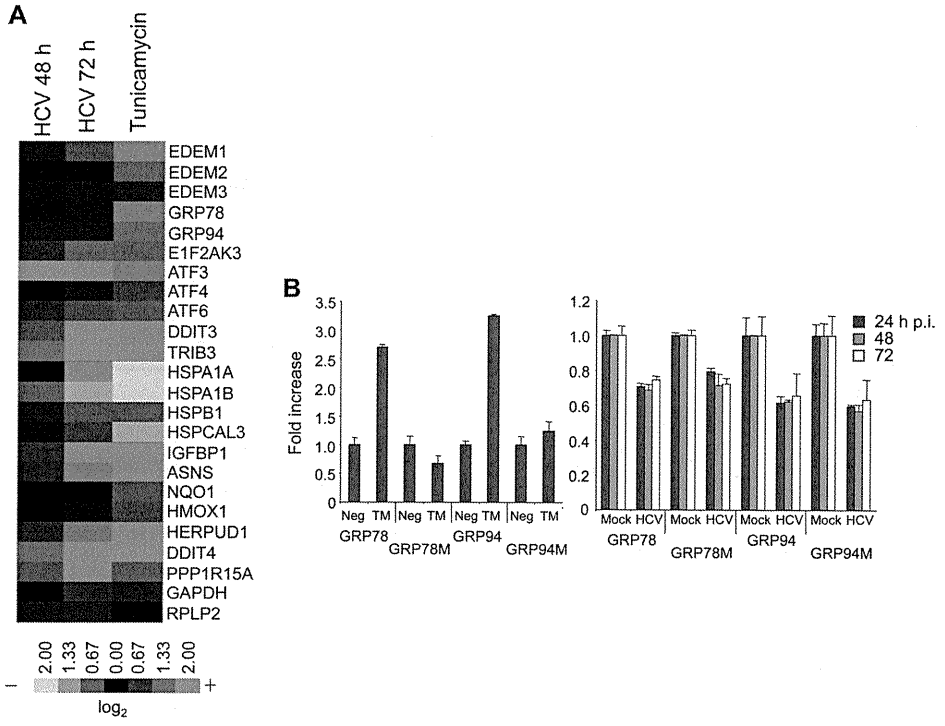

FIGURE 2. **Comprehensive analysis of ERAD gene expression in JFH-1-infected HuH-7.5.1 cells.** *A*, HuH-7.5.1 cells treated with TM (5 μg/ml) for 12 h or infected with JFH-1 for 48 and 72 h were subjected to microarray analysis, along with their negative controls. Expression of ER stress genes is shown as a heat map. *Red* and *green* indicate up- and down-regulation, respectively. Information on each gene shown is indicated on the 3D-Gene web site. *B*, GRP78 and GRP94 induction in TM-treated (*left*) and HCV-infected cells (*right*). GRP78M and GRP94M represent the defective promoters. The mean ± S.D. (*error bars*) of three independent experiments are shown.

packaging system of HCV subgenomic replicon sequences through the provision of viral core NS2 proteins in *trans* (19). Transcomplementation with core NS2 proteins resulted in successful packaging of the viral sequences; therefore, plasmids carrying these proteins are a valid construct by which to examine the interaction of envelope proteins with ERAD machinery. Thus, we performed an immunoprecipitation assay of HuH-7 cells co-transfected with core NS2 and EDEMs. In agreement with our previous results, EDEMs, but not ER ManI, were observed to bind to HCV E2 protein (supplemental Fig. S3*B*). To examine the functional importance of this interaction, we analyzed the ubiquitylation of HCV E2 protein in cells co-transfected with HCV E2 and EDEM proteins. An immunoprecipitation assay revealed that overexpression of EDEM1 and EDEM3, but not of EDEM2 and ER ManI, dramatically increased the ubiquitylation of HCV glycoprotein (Fig. 3*B*). In mammals, the ER membrane ubiquitin-ligase complex involved in the dislocation of ERAD substrates, and their ubiquitylation contains the ER membrane adaptor SEL1L. It has recently been shown that SEL1L interacts with EDEM1 in cells and functions as a cargo receptor for ERAD substrates (20); however, it is unknown whether SEL1L interacts with other EDEMs. We therefore assessed whether SEL1L interacts with EDEM1, EDEM2, EDEM3, and ER ManI in cells (Fig. 3*C*). Interestingly, endogenous SEL1L co-precipitated with EDEM1 and EDEM3, whereas little to no interaction was observed with EDEM2 and ER ManI. Collectively, it is likely that, although all EDEMs can recognize HCV E1 and E2, EDEM1 and EDEM3 are involved in the ubiquitylation of HCV glycoproteins by delivering them to SEL1L-containing ubiquitin-ligase complexes. To investigate further the role of EDEMs in quality control of HCV glycoproteins, we measured the steady-state level of HCV E2 protein after EDEM knockdown. Transfection of HCV-infected cells with siRNAs against EDEM1, EDEM2, or EDEM3 caused a 60–80% reduction in mRNA levels of the respective genes (Fig. 3*D*) with no cytotoxic effects observed (data not shown). Immunoblotting showed a considerable increase in the steady-state level of viral E2 in EDEM1 siRNA-treated cells (Fig. 3*D*). We subsequently examined the turnover of E2 in cells with and without EDEM1 knockdown. In CHX half-life experiments, E2 protein was moderately unstable in control-infected cells, presumably via proteasomal degradation (Fig. 3*E*). Treatment with MG132, a proteasome inhibitor, blocked its destabilization (data not shown). In contrast, E2 was completely stable in EDEM1-knockdown cells during the chase period of time tested (Fig. 3*E*). Together, these results strongly suggest that EDEM1 and EDEM3, particularly EDEM1, are involved in the post-translational control of HCV glycoproteins.

Involvement of EDEM1 in the Production of Infectious HCV—Given the involvement of EDEMs in the turnover of HCV glycoproteins, we investigated whether EDEMs affect the replication and production of infectious virus particles. EDEMs were knocked down in HCV-infected HuH-7 cells by siRNA transfection, and the production of infectious particles was then monitored by measuring the extracellular infectivity titer. Knocking down of EDEM1 and EDEM3 in the infected cells resulted in ~3.1-fold ($p < 0.05$) and ~2.3-fold increases in virus production, respectively, compared with control cells. No effect

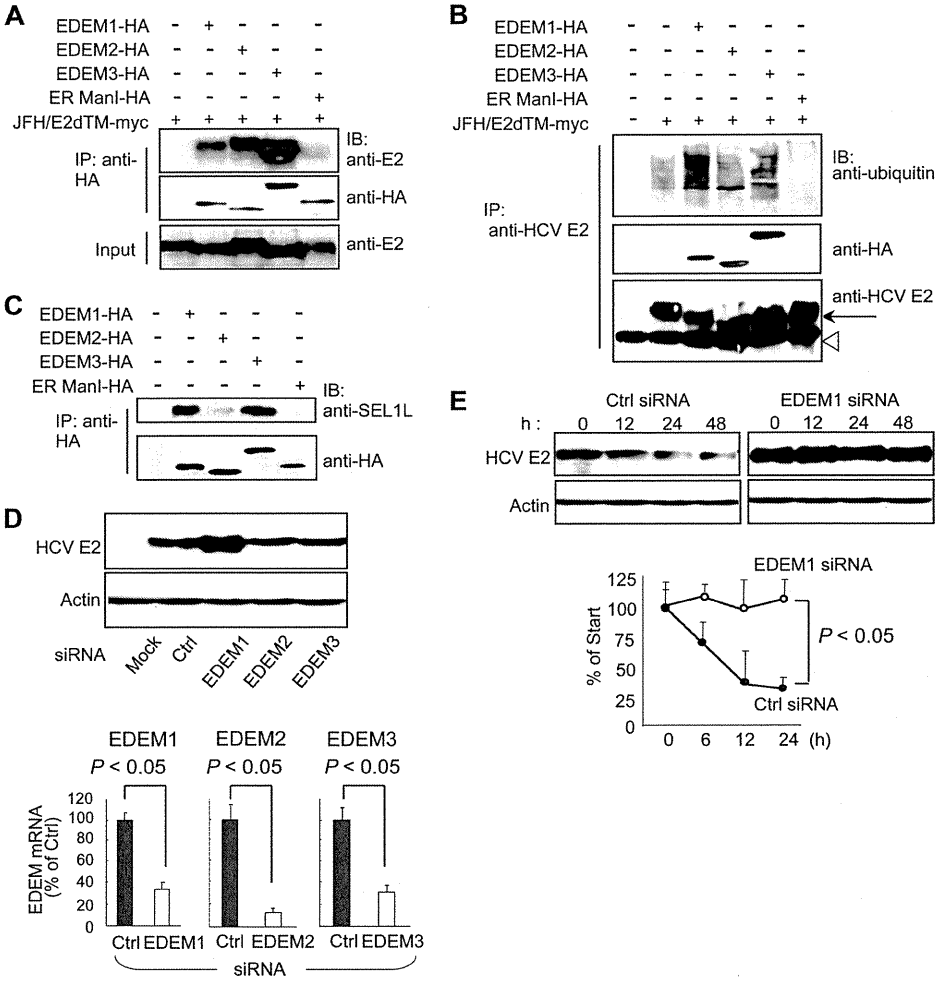

FIGURE 3. **EDEMs are involved in the degradation of HCV glycoproteins.** *A*, binding of EDEMs and ER ManI with HCV E2. 293T cells were seeded in 6-well plates at a density of 3×10^5 cells/well. After overnight incubation, cells were co-transfected with plasmids carrying HCV E2-myc (1 μg) and EDEM1-HA, EDEM2-HA, EDEM3-HA, or ER ManI-HA proteins (1 μg each). Forty-eight hours later, cells were harvested, immunoprecipitated (*IP*) with anti-HA antibodies, and Western blotting (*IB*) was performed with the indicated antibodies. *B*, ubiquitylation of HCV E2 protein in cells co-transfected with HCV E2 and EDEM plasmids. 293T cells were seeded in 6-well plates at a density of 3×10^5 cells/well. Twenty-four hours later, the cells were co-transfected with plasmids carrying HCV E2-myc (1 μg) and EDEM1-HA, EDEM2-HA, EDEM3-HA, or ER ManI-HA genes (1 μg each). Forty-eight hours later, the cells were harvested and immunoprecipitated with anti-E2 antibodies, and Western blotting was performed with the indicated antibodies. *Arrow*, HCV E2; *open arrowhead*, immunoglobulin heavy chain. *C*, binding of EDEMs and ER ManI with endogenous SEL1L in cells. *D*, steady-state level of HCV E2 in HCV-infected HuH-7 cells after EDEM knockdown (*upper*). The knockdown efficiencies of the respective siRNAs are shown in the *lower panel*. Values are normalized to GAPDH expression levels, and normalized values in negative control cells have been arbitrarily set at 100%. *E*, stability of HCV E2 protein in EDEM1 knockdown cells. HCV-infected HuH-7 cells were transfected with control or EDEM1 siRNA. Forty hours later, the cells were exposed to CHX (100 μg/ml) for 0, 12, 24, and 48 h, followed by immunoblotting. Specific signals were quantified by densitometry, and the percent of HCV E2 remaining was compared with initial levels. The mean ± S.D. (*error bars*) of two independent experiments are shown.

on virus production was observed following EDEM2 gene silencing (Fig. 4*A*). On the other hand, no significant differences were observed with regard to intracellular HCV core protein levels among mock- and EDEM siRNA-transfected cells (Fig. 4*B*), which indicates that replication of the viral genome is not affected by EDEM proteins. To examine further whether this effect on virus production was due to turnover of HCV envelope proteins, we performed loss-of-EDEM-function experiments in HuH-7 cells carrying HCV subgenomic replicons. Because the replicons do not require envelope proteins, they should be insensitive to the expression levels of genes involved in the ERAD pathway. As expected, siRNA-mediated knockdown of EDEMs resulted in little to no change in genome replication (supplemental Fig. S4*A*). To investigate further the participation of EDEMs in the HCV life cycle, HCV-infected cells were examined 48 h after transfection with an expression plasmid for either EDEM1, EDEM2, or EDEM3. As expected, exogenous expression of EDEM1 in the infected cells led to a 2.4-fold decrease in virus production compared with mock-transfected cells ($p < 0.05$) (Fig. 4*C*). A moderate decrease of 1.7-fold was observed in the cells overexpressing EDEM3 protein. Ectopic expression of EDEMs and ER ManI did not cause any change in intracellular HCV core protein levels (Fig. 4*D*). Similarly, little or no change was observed in genome replication when plasmids carrying EDEMs were introduced into HCV subgenomic replicon cells (supplemental Fig. S4*B*). These results indicate that EDEM1 and EDEM3, particularly EDEM1, regulate virus production, possibly through post-translational control of HCV glycoproteins.

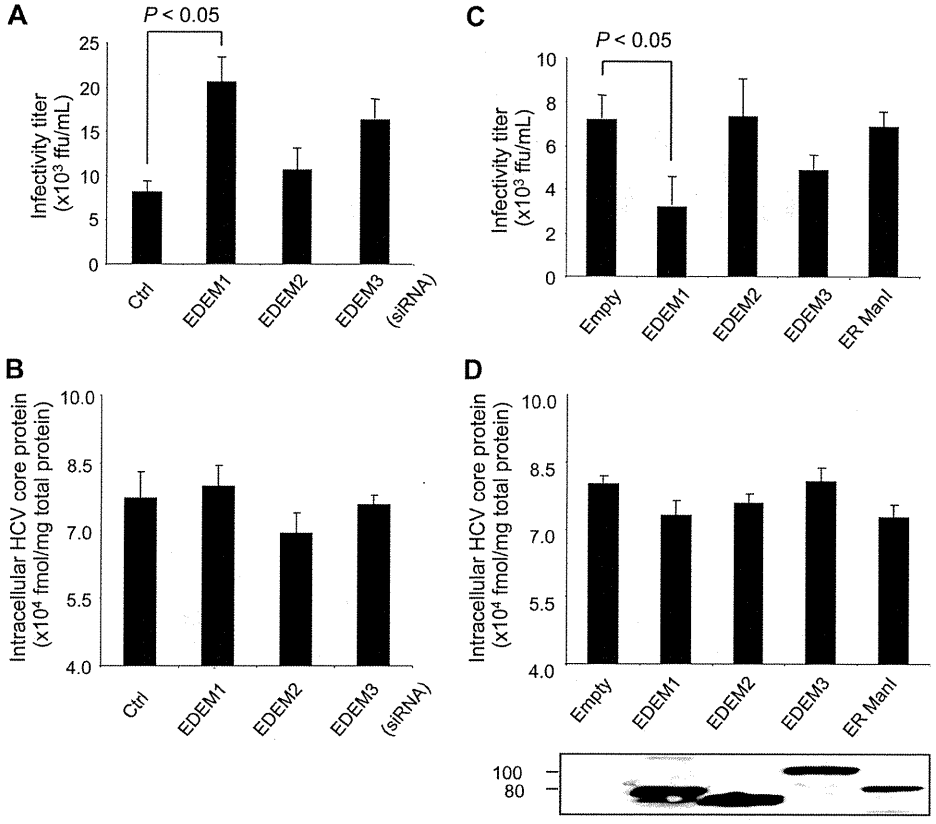

FIGURE 4. **Role of EDEMs in HCV replication and production of infectious virus particles.** *A*, HCV production in HuH-7 cells transfected with EDEM siRNAs. Cells were infected with JFH-1 at a m.o.i. of 1. Twenty-four hours later, the cells were transfected with the indicated siRNAs at a final concentration of 10 nM. The culture medium was harvested 48 h later and was used to infect naïve HuH-7.5.1 cells seeded in a 96-well plate. Immunostaining using anti-HCV core antibodies was performed at 72 h after infection, and focus-forming units were counted. *B*, siRNA-transfected and HCV-infected cells described in *A* harvested at 48 h after infection. Intracellular HCV core protein was measured. The values were normalized to total protein in the cell lysate samples. *C*, HCV production in HuH-7 cells transfected with plasmids carrying EDEM1-HA, EDEM2-HA, EDEM3-HA, or ER ManI-HA genes. *D*, intracellular HCV core protein within the cells described in *C*. Expression levels of the EDEMs and ER ManI were determined by anti-HA immunoblotting. The mean ± S.D. (*error bars*) of three independent experiments are shown in all of the *panels*.

Chemical Inhibition of the ERAD Pathway Increases HCV Production—KIF, a potent inhibitor of ER mannosidase, is reported to inhibit the ERAD pathway. When HCV-infected cells were treated with KIF, virus production increased in the culture medium in a dose-dependent manner (Fig. 5*A*, *left*), and the steady-state level of E2 in the cells increased accordingly (Fig. 5*A*, *right*). No change was observed in intracellular HCV core protein levels after KIF treatment (Fig. 5*A*, *center*). Kinetic analyses showed that E2 was stabilized dramatically in KIF-treated cells (Fig. 5*B*), whereas the fate of HCV core protein, a nonglycoprotein, was not affected by KIF treatment (supplemental Fig. S5). No effect on virus replication was observed when the cells harboring JFH-1 subgenomic replicons were treated with KIF (data not shown).

On the basis of these findings, one may hypothesize that KIF contributes to the stabilization of HCV glycoprotein(s) by interfering with the interaction between (i) EDEMs and viral proteins, or (ii) EDEMs and SEL1L. To address this, HCV E2 was co-expressed in 293T cells with EDEM1, EDEM2, EDEM3, or ER ManI in the presence or absence of KIF, followed by immunoprecipitation (Fig. 5*C*). E2 was shown to interact with EDEM1, EDEM2, and EDEM3, analogous to the data shown in Fig. 3*A*, and KIF did not block the interactions. Decreased electrophoretic mobility of E2 was detected in KIF-treated cells, possibly due to a change in glycan composition caused by inhibition of mannosidase activity. These findings led us to investigate whether the glycans on HCV glycoproteins are required for binding to EDEMs. We generated E1 and E2 mutants by replacing their *N*-glycosylation sites with glutamine residues and analyzed their interaction with EDEMs. Removal of the glycans did not inhibit the binding of E1 and E2 proteins to EDEM, demonstrating that *N*-glycans on the surface of viral proteins are not indispensible for an interaction between EDEMs and HCV glycoproteins to occur (supplemental Fig. S6). The effect of KIF on the association of EDEMs with downstream ERAD machinery was examined further. In cells co-expressing E2 and EDEMs, the interaction of SEL1L with EDEM1 and EDEM3 was significantly reduced in the presence of KIF ($p < 0.05$) (Fig. 5*C*). Consistent with these results, KIF abrogated the EDEM1- and EDEM3-mediated ubiquitylation of HCV E2 protein (Fig. 5*D*). This inhibitory effect of KIF on the SEL1L-EDEM interaction was also observed in HuH-7 cells (supplemental Fig. S7). These results suggest that KIF stabilizes HCV glycoproteins by interfering with the SEL1L-EDEM interaction and thus leads to an increase in virus production.

Role of ERAD in the Life Cycle of JEV—This study demonstrates involvement of the ERAD pathway in HCV production. However, the role of this pathway in the production of other

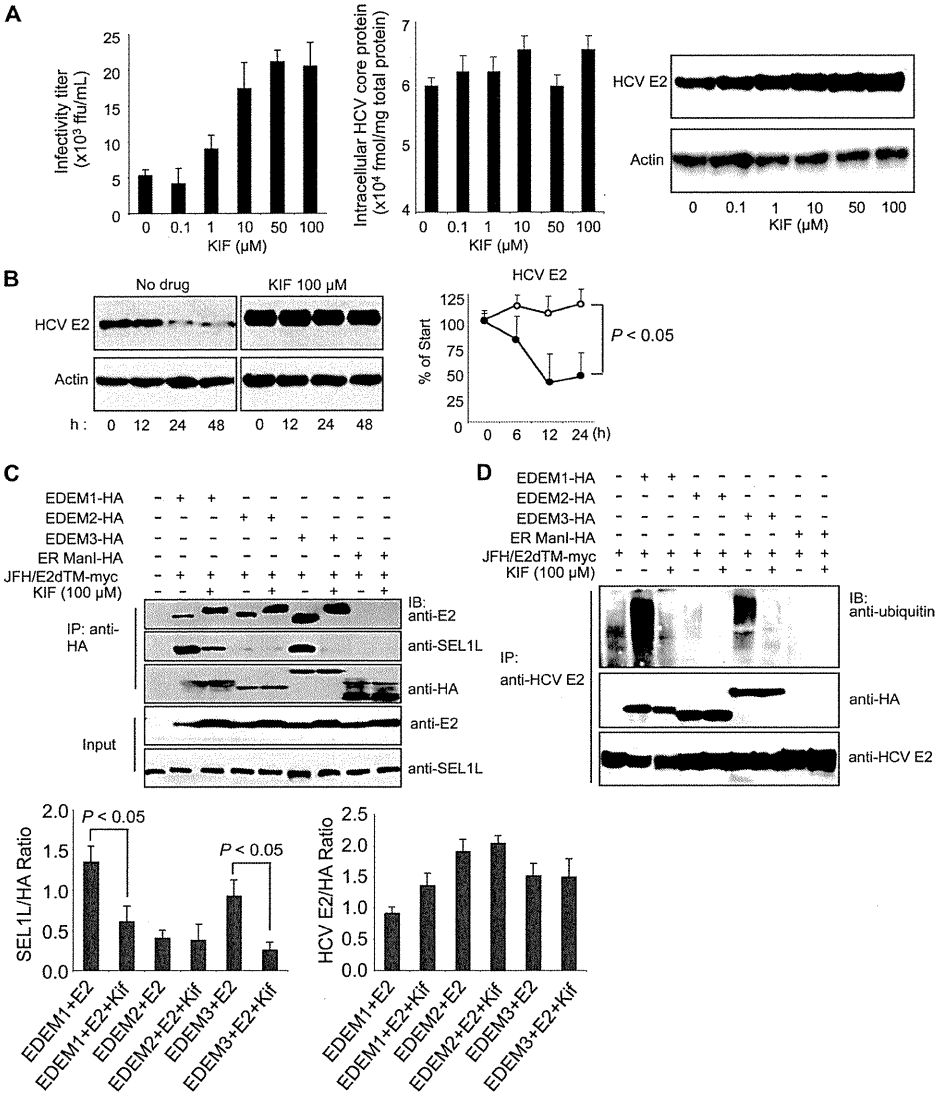

FIGURE 5. **Effect of KIF on HCV production and stability of E2.** *A*, extracellular HCV titer, intracellular HCV core protein expression, and steady-state level of HCV E2 in HuH-7 cells treated with different concentrations of KIF. *B*, CHX-based HCV protein stability assay of HCV E2 protein in KIF-treated cells as described in Fig. 3*E*. E2 protein levels normalized to actin levels are shown in the *graph* on the *right*. The *open* and *filled circles* indicate KIF-treated and nontreated cells, respectively. The mean ± S.D. (*error bars*) of two independent experiments are shown. *C*, binding of EDEMs and ER ManI with HCV E2 and SEL1L in 293T cells in the absence or presence of KIF. 293T cells were seeded in 6-well plates at a density of 3×10^5 cells/well. After overnight incubation, the cells were co-transfected with plasmids carrying HCV E2-myc (1 μg) and EDEM1-HA, EDEM2-HA, EDEM3-HA, or ER ManI-HA proteins (1 μg each). After 6 h, the culture medium was replaced with fresh or KIF-containing medium (100 μM). Forty-eight hours later, the cells were harvested and immunoprecipitated (*IP*) with anti-HA antibodies, after which Western blotting (*IB*) was performed with the indicated antibodies. Specific signals were quantified by densitometry, and the ratio between HCV E2 and HA (*right graph*) and between SEL1L and HA (*left graph*) in the same *lanes* is plotted on the graphs. The mean ± S.D. of three independent experiments are shown. *D*, EDEM protein-mediated ubiquitylation of HCV E2 protein in 293T cells in the absence or presence of KIF. The experimental procedure was the same as that described in Fig. 5*C*, except that immunoprecipitation was performed with anti-HCV E2 antibodies.

viruses is still unknown. To this end, we examined its role in the life cycle of JEV, another member of the Flaviviridae family. In contrast to HCV, KIF treatment had little effect on JEV production in infected cells (Fig. 6*A*) or the steady-state level of viral E glycoprotein (Fig. 6*B*). Interaction of EDEMs with JEV E was analyzed further. Neither EDEMs nor ER ManI was found to interact with JEV E in cells (Fig. 6*C*), indicating no significant role of the ERAD pathway in the JEV life cycle. Altogether, these results strongly suggest that the ERAD pathway is involved in the quality control of glycoproteins of specific viruses, possible through an interaction with EDEM(s), and subsequent regulation of virus production.

DISCUSSION

Accumulating evidence points to a role of the ERAD pathway in the pathogenesis of different genetic and degenerative diseases. However, the involvement of ERAD in the life cycle of viruses and infectious diseases remains poorly understood. Until recently, an experimental HCV cell culture infection system has been lacking such that studies evaluating the effect of HCV infection on the ERAD pathway were performed by either using HCV subgenomic replicons which lack structural proteins or by ectopic expression of one or multiple structural proteins (21, 22). However, this problem was solved by identifica-